THE JOURNAL OF PHYSICAL CHEMISTRY A
A JOURNAL OF THE AMERICAN CHEMICAL SOCIETY

pubs.acs.org/JPCA

Review Article

How to VPT2: Accurate and Intuitive Simulations of CH Stretching Infrared Spectra Using VPT2+K with Large Effective Hamiltonian Resonance Treatments

Peter R. Franke, John F. Stanton, and Gary E. Douberly*

Cite This: J. Phys. Chem. A 2021, 125, 1301−1324

Read Online

ACCESS | Metrics & More | Article Recommendations | Supporting Information

ABSTRACT: This article primarily discusses the utility of vibrational perturbation theory for the prediction of X−H stretching vibrations with particular focus on the specific variant, second-order vibrational perturbation theory with resonances (VPT2+K). It is written as a tutorial, reprinting most important formulas and providing numerous simple examples. It discusses the philosophy and practical considerations behind vibrational simulations with VPT2+K, including but not limited to computational method selection, cost-saving approximations, approaches to evaluating intensity, resonance identification, and effective Hamiltonian structure. Particular attention is given to resonance treatments, beginning with simple Fermi dyads and gradually progressing to arbitrarily large polyads that describe both Fermi and Darling−Dennison resonances. VPT2+K combined with large effective Hamiltonians is shown to be a reliable framework for modeling the complicated CH stretching spectra of alkenes. An error is also corrected in the published analytic formula for the VPT2 transition moment between the vibrational ground state and triply excited states.

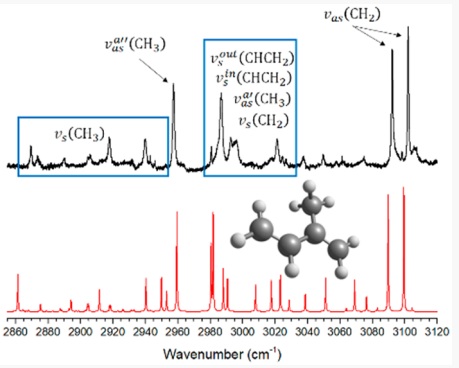

1. INTRODUCTION

1.1. Theoretical Computation of Infrared Spectra. Most simulations of vibrational spectra begin with determination of the normal modes of vibration and application of the harmonic oscillator approximation.[1,2] This approximation entails that the potential energy surface (PES) is a quadratic function of $3N - 6$ (or $3N - 5$ if linear) uncoupled normal coordinates. A similar approximation is made to the dipole moment surface (DMS), which governs the intensity of infrared absorption. It is taken to be a linear function of the normal coordinates. Together these assumptions comprise the "double harmonic" approximation. This approach is most successful for molecules with well-defined equilibrium structures, lacking low-frequency vibrations, and having low degrees of vibrational excitation, such that their vibrational motions do not carry them far from the equilibrium structure. The necessary terms in the PES and DMS can respectively be expressed as second derivatives of the electronic energy and first derivatives of the dipole moment, with respect to normal coordinate displacements. Alternatively, first derivatives of the dipole moment are equivalent to second derivatives of the electronic energy with respect to both applied electric field and normal coordinate displacements. A version of the harmonic analysis is implemented in all major quantum chemistry programs; however, the electronic structure methods that support it usually depend on the availability of analytic energy derivatives.

In order to achieve quantitative accuracy, descriptions of molecular vibration beyond the harmonic approximation are necessary. Methods of treating this "anharmonicity", in a harmonic oscillator basis, include vibrational perturbation theory (VPT) and variational approaches, both based on Taylor series expansions of the potential.[3] The vibrational self-consistent field (VSCF) method[4] is an alternative, which variationally improves the zeroth-order wave functions. Further corrections are then typically made to the VSCF wave functions, which are analogous to the MP2, CI, and CC treatments of electron correlation.

1.2. Challenges Associated with Nonrigid Molecules. Nonrigidity (or floppiness) is the condition in which a system may explore large amounts of its nuclear configuration space in the vibrational ground state. Such a thing is also referred to as large-amplitude motion (LAM), contrasting with the small-amplitude motion of (mostly) harmonic oscillators vibrating about a well-defined equilibrium structure.[1] One consequence of LAM is that it often gives rise to multiple conformers,

Received: October 21, 2020
Revised: January 12, 2021
Published: January 28, 2021

complicating (or perhaps enriching) interpretation of spectral patterns.

In theoretical chemistry, a small to moderate amount of LAM leads to increased errors in the harmonic oscillator model and in anharmonic models that build upon it, such as VPT. Although much of the error is often found to be isolated in the low-frequency normal coordinates, predictions of reasonable but diminished quality may still be made for high-frequency vibrations, as seen with floppy alkyl radicals.[5] The *n*-propyl and *i*-propyl radicals have low barriers to torsional and wagging motions, respectively, localized on their radical sites. They also feature one and two methyl tops, respectively, which are notorious for undergoing weakly hindered rotation. Reduced-dimensionality schemes (i.e., VPT based on a force field that neglects low-frequency coordinates) have sometimes been used in attempts to ameliorate the errors.[6,7] In the experience of the authors, reduced dimensionality schemes seldom lead to higher-accuracy predictions for the high-frequency vibrations. More sophisticated ways of correcting for LAM have been described,[8] but such methods are not widely implemented and tend to be greatly more complicated than standard VPT. In the case of severe LAM, such as in proton-bound dimers,[9,10] errors become catastrophic, and the normal-mode harmonic oscillator starting point should be abandoned in favor of descriptions based on curvilinear internal coordinates and more expansive potential energy surfaces, such as discrete variable representation approaches[11] or extensions of VSCF.[12]

In certain cases of LAM, a situation arises in which the electronic PES has multiple minima separated by a sufficiently shallow barrier, such that the ground state wave function is highly delocalized, with the largest amplitude above the barrier.[13] Similarly, it can sometimes be shown that correction for zero-point vibrational energy (ZPVE) merges the shallow multiple-well features into a single well.[14] In these cases, although the PES holds several wells, these likely do not correspond to conformers. The equilibrium structures cease to be meaningful, and although one might be tempted to carry out an anharmonic analysis at the transition state structure (i.e., at the top of the barrier), this is not a straightforward procedure for most methods (e.g., VPT).[14]

2. METHODS

2.1. Introduction to Vibrational Perturbation Theory. Second-order vibrational perturbation theory (VPT2) is an old and widely used method for dealing with anharmonicity in molecular vibrations.[3,15] Anharmonicity is defined as the deviation of vibrations from the harmonic model. In standard applications of perturbation theory, the Hamiltonian is separated into a zeroth-order part, the exact eigenfunctions of which are known, and a perturbation that is assumed to be small. The common, analytic formulation of VPT is based on the Watson Hamiltonian; accordingly, it uses a rectilinear normal coordinate system.[16−18] This means that the vibrational displacement coordinates are linear combinations of Cartesian coordinates, and atoms move in straight (as opposed to curved) paths. The implications of this fact are far-reaching; however, that is beyond the scope of this discussion.[19] The zeroth-order part of the vibrational Hamiltonian corresponds to the harmonic oscillator Hamiltonian, which is based on a quadratic expansion of the potential energy surface, and the perturbation is the anharmonic potential. The effects of vibrational angular momentum are also normally included, again as a perturbation. Moreover, computations are typically performed for $J = 0$, allowing for the neglect of Watson Hamiltonian terms, which involve powers of the rotational angular momentum operator. It is common to subdivide the perturbation into numbered Hamiltonians, and this will soon make it more clear what kinds of terms can contribute to each part of the energy expression.[20]

$$\begin{aligned}\hat{H} &= \hat{H}_0 + \hat{H}' \\ &= \hat{H}_{\mathrm{HO}} + \hat{V}_{\mathrm{anh}} + \hat{H}_{\mathrm{cor}} + \hat{U} \\ &= \hat{H}_{\mathrm{HO}} + \hat{H}_1 + \hat{H}_2\end{aligned} \tag{1}$$

For convenience, the normal coordinates are additionally made dimensionless, and most of the involved parameters (harmonic frequencies, anharmonic force constants, and rotational constants) are expressed in wavenumbers. The anharmonic potential energy is represented by a Taylor series expansion in the normal coordinates,

$$\begin{aligned}\hat{V}_{anh} = &\frac{1}{3!}\sum_{rst}\phi_{rst}\hat{q}_r\hat{q}_s\hat{q}_t + \frac{1}{4!}\sum_{rstu}\phi_{rstu}\hat{q}_r\hat{q}_s\hat{q}_t\hat{q}_u \\ &+ \frac{1}{5!}\sum_{rstuv}\phi_{rstuv}\hat{q}_r\hat{q}_s\hat{q}_t\hat{q}_u\hat{q}_v + \ldots\end{aligned} \tag{2}$$

where the factors of $1/n!$ are Taylor series coefficients; r, s, t, u, v are normal coordinates; $\hat{q}_r, \hat{q}_s, \hat{q}_t, \hat{q}_u, \hat{q}_v$ are the associated position operators; and ϕ_{rst} is a cubic force constant,

$$\phi_{rst} = \left(\frac{\partial^3 E}{\partial q_r \partial q_s \partial q_t}\right) \tag{3}$$

a third derivative of the electronic energy with respect to displacement along coordinates r, s, t. Note the summation is unrestricted, so force constants where $r, s,$ and/or t refer to the same coordinate will appear. Also, there are six equivalent permutations of r, s, t; three equivalent permutations of r, s, s; and only one permutation of r, r, r. This redundancy is accounted for by introducing degeneracy factors. Analogously, ϕ_{rstu} is a quartic force constant, and ϕ_{rstuv} is a quintic force constant. The quartic force constants (and all higher force constants) have similar definitions.

$$\phi_{rstu} = \left(\frac{\partial^4 E}{\partial q_r \partial q_s \partial q_t \partial q_u}\right) \tag{4}$$

2.2. Harmonic Oscillator Integrals. The harmonic oscillator Hamiltonian, $\hat{H}_{\mathrm{HO}}$, is of course diagonal in the harmonic oscillator basis set and its eigenvalues are simply linear combinations of the $3N-6$ (or $3N-5$) harmonic frequencies of the system. A great advantage of anharmonic approaches that use the traditional rectilinear normal coordinate system and harmonic oscillator basis set is the ease of integral evaluation. The matrix elements of the normal coordinate position, $\hat{q}$, and momentum, $\hat{p}$, operators, which appear in the anharmonic terms, have simple analytic formulas, which are published in various texts.[1,2] In order to determine the VPT2 energy, matrix elements are required in which the exponent of the $\hat{q}$ operator ranges from 0 to 4. Integrals involving products of position and momentum operators also appear in the vibrational angular momentum terms. Many of these are not required in VPT2, as only the diagonal vibrational angular momentum matrix elements are included. Furthermore, these integrals can all be rewritten in terms of position integrals.[21] The harmonic oscillator position integrals up to the fourth power are provided below.

https://dx.doi.org/10.1021/acs.jpca.0c09526
J. Phys. Chem. A 2021, 125, 1301−1324

$$\langle n'|n\rangle = \delta_{n',n} \tag{5}$$

$$\langle n'|\hat{q}|n\rangle = \frac{1}{\sqrt{2}}[\delta_{n',n-1}\sqrt{n} + \delta_{n',n+1}\sqrt{n+1}] \tag{6}$$

$$\langle n'|\hat{q}^2|n\rangle = \frac{1}{2}[\delta_{n',n-2}\sqrt{n(n-1)} + \delta_{n',n}(2n+1) + \delta_{n',n+2}\sqrt{(n+1)(n+2)}] \tag{7}$$

$$\langle n'|\hat{q}^3|n\rangle = \frac{1}{2\sqrt{2}}[\delta_{n',n-3}\sqrt{n(n-1)(n-2)} + \delta_{n',n-1}(3n^{3/2}) + \delta_{n',n+1}(3(n+1)^{3/2}) + \delta_{n',n+3}\sqrt{(n+1)(n+2)(n+3)}] \tag{8}$$

$$\langle n'|\hat{q}^4|n\rangle = \frac{1}{4}[\delta_{n',n-4}\sqrt{n(n-1)(n-2)(n-3)} + \delta_{n',n-2}(4n-2)\sqrt{n(n-1)} + \delta_{n',n}(6n^2+6n+3) + \delta_{n',n+2}(4n+6)\sqrt{(n+1)(n+2)} + \delta_{n',n+4}\sqrt{(n+1)(n+2)(n+3)(n+4)}] \tag{9}$$

In these expressions, δ is the Kronecker delta, $\hat{q}$ is the position operator associated with a particular normal coordinate, and the indices n and n' are the number of quanta of excitation in that coordinate. The harmonic oscillator integrals are straightforwardly solved for within the raising/lowering operator formalism where

$$\hat{a}^\dagger|n\rangle = \sqrt{n+1}\,|n+1\rangle \tag{10}$$

$$\hat{a}|n\rangle = \sqrt{n}\,|n-1\rangle \tag{11}$$

shows the result of operating on an arbitrary vibrational state, $|n\rangle$, with the raising and lowering operators, respectively. In this formalism, the position and momentum operators respectively adopt the following forms:

$$\hat{q} = \frac{1}{\sqrt{2}}(\hat{a} + \hat{a}^\dagger) \tag{12}$$

$$\hat{p} = -\frac{\mathrm{i}}{\sqrt{2}}(\hat{a} - \hat{a}^\dagger) \tag{13}$$

The harmonic oscillator integrals can be solved by successive application of raising and lowering operators to an arbitrary vibrational state. Returning to the vibrational Hamiltonian, $\hat{H}_1$ is the cubic potential operator that can be expressed as follows:

$$\hat{H}_1 = \frac{1}{6}\sum_{rst}\phi_{rst}\hat{q}_r\hat{q}_s\hat{q}_t \tag{14}$$

Similarly, $\hat{H}_2$ contains the quartic potential, the vibrational angular momentum, and the so-called Watson pseudopotential, which makes a small mass-dependent contribution.

$$\hat{H}_2 = \frac{1}{24}\sum_{rstu}\phi_{rstu}\hat{q}_r\hat{q}_s\hat{q}_t\hat{q}_u + \hat{H}_{\mathrm{cor}} + \hat{U} \tag{15}$$

The relevant (diagonal) part of the vibrational angular momentum can be written as

$$\hat{H}_{\mathrm{cor}} = \sum_{\tau,s>r}\left[\left(\frac{\omega_r^2 + \omega_s^2}{\omega_r\omega_s}\right)B_{\mathrm{e}}^{\tau}(\zeta_{rs}^{\tau})^2\right]\hat{q}_r^{\,2}\hat{q}_s^{\,2} \tag{16}$$

where τ runs over the inertial axes, ω_r represents the harmonic frequency of normal coordinate r, B_{e}^{τ} is the equilibrium rotational constant associated with the τ axis, and ζ is a Coriolis constant.[21] Coriolis constants are unitless and are interpreted as follows: ζ_{rs}^{a} couples normal coordinates r and s via a rotation about the a inertial axis. The lowest-order pseudopotential term can be written simply as

$$\hat{U} = -\frac{1}{4}\sum_{\tau}B_{\mathrm{e}}^{\tau} \tag{17}$$

i.e., a sum over the equilibrium rotational constants. The pseudopotential makes only a constant contribution to the energy at VPT2, so it may be ignored in determining transition frequencies.

2.3. Sum-over-States VPT2. The standard expression for the energy of state a, to second-order in perturbation theory, is given below.

$$E_{\mathrm{a}} = \langle a|\hat{H}_0|a\rangle + \langle a|\hat{H}'|a\rangle + \sum_{b\neq a}\left(\frac{\langle a|\hat{H}'|b\rangle\langle b|\hat{H}'|a\rangle}{\langle a|\hat{H}_0|a\rangle - \langle b|\hat{H}_0|b\rangle}\right) \tag{18}$$

This formulation of VPT2 will be referred to as sum-over-states (SoS) VPT2. The sum runs over all zeroth-order states, of which there are an infinite number. This can be simplified first by introducing

$$\epsilon_a = \langle a|\hat{H}_{\mathrm{HO}}|a\rangle \tag{19}$$

$$E_{\mathrm{a}} = \epsilon_a + \langle a|\hat{H}'|a\rangle + \sum_{b\neq a}\frac{\langle a|\hat{H}'|b\rangle\langle b|\hat{H}'|a\rangle}{\epsilon_a - \epsilon_b} \tag{20}$$

choosing ϵ instead of ω to represent the energy of any arbitrary harmonic state. The definition of "orders" of vibrational perturbation theory is somewhat unconventional. Ordinarily, only the terms in the perturbation expansion are considered to have "orders". From left to right, the terms in the VPT2 energy expression are zeroth-, first-, and second-order. However, in VPT, also the orders of the various terms in the Hamiltonian are considered. The order of each term is given by its total number of position and momentum operators minus two. Accordingly, $\hat{H}_1$, the first-order Hamiltonian, contains first-order terms, and $\hat{H}_2$ contains second-order terms. The overall order of the Hamiltonian and perturbation theory correction determines what terms contribute to each order of VPT.[20,22] A motivation for these definitions of perturbation orders is the fact that all odd-order potential terms could make contributions to the second-order perturbation theory term; likewise, all even-order potential terms could contribute to the first-order perturbation theory term. Note that the pseudopotential is an exception to the rules for determining order, as when it makes its first contribution to the second-order Hamiltonian, it contains no position or momentum operators. Moreover, when determining the orders of Hamiltonian terms in rovibrational calculations, each instance of the rotational angular momentum operator should be counted as well (e.g., the rigid rotor term is zeroth-order).

The harmonic approximation can be considered VPT0. Only the zeroth-order term involving the zeroth-order Hamiltonian operator appears. VPT1 introduces the first-order perturbation theory term, which is a diagonal correction; however, only first-

https://dx.doi.org/10.1021/acs.jpca.0c09526
J. Phys. Chem. A 2021, 125, 1301−1324

order operators may contribute to this. Upon inspection of the terms in the first-order Hamiltonian, $\hat{H}_1$, three sets of rules become apparent.

For $\phi_{rrr}\hat{q}_r^{\,3} = \phi_{iii}\langle r|\hat{q}_r^{\,3}|r'\rangle$,

$\Delta n_r = \pm 1, \pm 3$ can be nonzero.

For terms $\phi_{rrs}\hat{q}_r^{\,2}\hat{q}_s = \phi_{rrs}\langle r|\hat{q}_r^{\,2}|r'\rangle\langle s|\hat{q}_s|s'\rangle$

$\Delta n_r = 0, \pm 2$, $\Delta n_s = \pm 1$ can be nonzero.

For terms $\phi_{rst}\hat{q}_r\hat{q}_s\hat{q}_t = \phi_{rst}\langle r|\hat{q}_r|r'\rangle\langle s|\hat{q}_s|s'\rangle\langle t|\hat{q}_t|t'\rangle$,

$\Delta n_r = \pm 1$, $\Delta n_s = \pm 1$, $\Delta n_t = \pm 1$ can be nonzero.

In these cases, Δn_r represents the number of quanta that is allowed to change in normal coordinate r. All of the diagonal matrix elements of the $\hat{H}_1$ operator must be zero; therefore, there is no first-order contribution to the VPT energy, and VPT1 would be no different from the harmonic approximation. It is important to note that when a $\hat{q}_r^n$ operator is absent from a term in $\hat{H}$, it corresponds to $\hat{q}_r^0$, which is the overlap integral/Kronecker delta. This means that the excitation level in other normal coordinates is not permitted to change.

Moving now to VPT2, the second-order perturbation theory term is introduced, which involves off-diagonal coupling matrix elements, but only the first-order Hamiltonian matrix elements are retained in it. In addition to this, now the second-order Hamiltonian is allowed to contribute to the first-order energy correction. The second-order perturbation theory terms including $\hat{H}_1$ involve off-diagonal matrix elements between arbitrary pairs of vibrational states, and there are many opportunities for these to be nonzero. For example, the terms of the form $\phi_{rrr}\hat{q}_r^{\,3}$ will allow $|r\rangle$ to couple to $|r+1\rangle$ and $|r+3\rangle$ but not to $|r+2\rangle$. More generally, the matrix elements will permit coupling between harmonic oscillator states that differ by either 1 or 3 net quanta. Can any of the first-order terms involving $\hat{H}_2$ be nonzero? Numerous types of quartic terms are contained in $\hat{H}_2$, and they obey the following five sets of rules.

For $\phi_{rrrr}\hat{q}_r^{\,4} = \phi_{rrrr}\langle r|\hat{q}_r^{\,4}|r'\rangle$,

$\Delta n_r = 0, \pm 2, \pm 4$ can be nonzero.

For $\phi_{rrss}\hat{q}_r^{\,2}\hat{q}_s^{\,2} = \phi_{rrss}\langle r|\hat{q}_r^{\,2}|r'\rangle\langle s|\hat{q}_s^{\,2}|s'\rangle$,

$\Delta n_r = 0, \pm 2$, $\Delta n_s = 0, \pm 2$ can be nonzero.

For $\phi_{rrrs}\hat{q}_r^{\,3}\hat{q}_s = \phi_{rrrs}\langle r|\hat{q}_r^{\,3}|r'\rangle\langle s|\hat{q}_s|s'\rangle$,

$\Delta n_r = \pm 1, \pm 3$, $\Delta n_s = \pm 1$ can be nonzero.

For $\phi_{rrst}\hat{q}_r^{\,2}\hat{q}_s\hat{q}_t = \phi_{rrst}\langle r|\hat{q}_r^{\,2}|r'\rangle\langle s|\hat{q}_s|s'\rangle\langle t|\hat{q}_t|t'\rangle$,

$\Delta n_r = 0, \pm 2$, $\Delta n_s = \pm 1$, $\Delta n_t = \pm 1$ can be nonzero.

For $\phi_{rstu}\hat{q}_r\hat{q}_s\hat{q}_t\hat{q}_u = \phi_{rstu}\langle r|\hat{q}_r|r'\rangle\langle s|\hat{q}_s|s'\rangle\langle t|\hat{q}_t|t'\rangle\langle u|\hat{q}_u|u'\rangle$,

$\Delta n_r = \pm 1$, $\Delta n_s = \pm 1$, $\Delta n_t = \pm 1$, $\Delta n_u = \pm 1$ can be nonzero.

The first two types of quartic terms can be nonzero when the number of quanta does not change. The rotation−vibration terms are analogous to the second type of quartic potential term, containing $\hat{q}_r^{\,2}\hat{q}_s^{\,2}$ operators, so they may also contribute to the VPT2 energy. None of the other quartic terms may contribute to the VPT2 energy. This fact is greatly advantageous. Although all cubic force constants are necessary to evaluate the VPT2 energy, no quartic force constants with three or four unique indices need to be known.

Thanks to the restrictive definition of VPT2 and the properties of the harmonic oscillator integrals, the energy expression simplifies further.

$$E_a = \epsilon_a + \langle a|\hat{H}_2|a\rangle + \sum_{b\neq a}\frac{\langle a|\hat{H}_1|b\rangle\langle b|\hat{H}_1|a\rangle}{\epsilon_a - \epsilon_b} \tag{21}$$

It was previously stated that only vibrational states differing by one or three net quanta can be coupled by $\hat{H}_1$. From this, it is clear that the sum over states can be truncated without any loss of accuracy. To determine the VPT2 energy of any vibrational state, it is sufficient to sum over only those vibrational states that are singly or triply excited or de-excited with respect to it. (Point group symmetry can impose further restrictions, as only states of the same symmetry may couple.) With these considerations, along with extensive algebra, the sum over vibrational states and all of the integrals can be eliminated from the VPT2 energy expression, rendering it down to an algebraic form with finite sums over the normal coordinates. It can then be arranged into a familiar, spectroscopic form.

2.4. The VPT2 Equations for Asymmetric Tops. Efficient VPT2 implementations are based on "anharmonicity constants". These are multidimensional analogues of the $\omega_e x_e$ term that appears in the Dunham expansion for the rovibrational energy of a diatomic molecule.[15,23] Given below is the Dunham expansion truncated at the first three pure vibrational terms.

$$E(\mathrm{v}) = \omega_e\left(\mathrm{v}+\frac{1}{2}\right) - \omega_e x_e\left(\mathrm{v}+\frac{1}{2}\right)^2 + \omega_e y_e\left(\mathrm{v}+\frac{1}{2}\right)^3 \tag{22}$$

The diagonal and off-diagonal anharmonicity constants are defined as follows.

$$\chi_{rr} = \frac{1}{16}\phi_{rrrr} - \frac{1}{32}\sum_s \phi_{rrs}^{\,2}\left(\frac{1}{2\omega_r+\omega_s} + \frac{4}{\omega_s} - \frac{1}{2\omega_r-\omega_s}\right) \tag{23}$$

$$\chi_{rs} = \frac{1}{4}\phi_{rrss} - \frac{1}{4}\sum_t \frac{\phi_{rrt}\phi_{sst}}{\omega_t} - \frac{1}{8}\sum_t \phi_{rst}^{\,2}\left(\frac{1}{\omega_r+\omega_s+\omega_t} + \frac{1}{-\omega_r+\omega_s+\omega_t} + \frac{1}{\omega_r-\omega_s+\omega_t} - \frac{1}{\omega_r+\omega_s-\omega_t}\right) + \sum_\tau B_e^\tau(\zeta_{rs}^\tau)^2\left(\frac{\omega_r}{\omega_s}+\frac{\omega_s}{\omega_r}\right) \tag{24}$$

The VPT2 energy can be defined in terms of the anharmonicity constants,

$$E(\mathrm{v}) = G_0 + \sum_r \omega_r\left(\mathrm{v}_r+\frac{1}{2}\right) + \sum_{r\geq s}\chi_{rs}\left(\mathrm{v}_r+\frac{1}{2}\right)\left(\mathrm{v}_s+\frac{1}{2}\right) \tag{25}$$

where v_r and v_s are the number of quanta in normal coordinates r and s, respectively. Additionally, the double sum has the condition that $s \geq r$. This results in equivalent anharmonicity constants χ_{rs} and χ_{sr} only being counted once. Calculating the energy of a vibrational state using this summation over anharmonicity constants is exactly equivalent to (but far more compact than) performing the sum-over-states with the second-order perturbation theory expression. Note the term G_0, which

https://dx.doi.org/10.1021/acs.jpca.0c09526
J. Phys. Chem. A 2021, 125, 1301−1324

collects all contributions to the energy that do not depend on the vibrational quantum numbers. Its evaluation is unnecessary when the goal is determination of transition frequencies; however, it is important for rigorous determination of the ZPVE.[24] The contribution of G_0 will be ignored in the ensuing discussion.

In principle, VPT2 can be applied to any molecule; however, linear molecules, symmetric tops, and spherical tops all have special formulas to correctly handle excitation in degenerate normal coordinates and the vibrational angular momentum that results.[2,25] While it is not rigorously correct to use the asymmetric top expressions for these systems of higher symmetry, other sources of error in the treatment (e.g., perturbation theory and quality of the potential surface) will usually dominate. Some of the structure of degenerate overtone bands is not recovered unless the proper equations are used, and this may be of concern to high-resolution spectroscopists. But because of the relative simplicity and ubiquity of the asymmetric top expressions, this discussion concerns only them.

Setting all v = 0 and allowing r to run over all $3N - 6$ normal coordinates would give the full anharmonic ZPVE (G_0 is neglected). Instead, ignore the sums over r and compute the ZPVE associated only with normal coordinate a.

(ia) Vibrational ground state (ZPVE) of normal coordinate a:

$$E_0 = \omega_a\left(\mathrm{v}_a + \frac{1}{2}\right) + \sum_s \chi_{as}\left(\mathrm{v}_a + \frac{1}{2}\right)\left(\mathrm{v}_s + \frac{1}{2}\right) \tag{26}$$

It will be helpful to distinguish terms involving diagonal and off-diagonal anharmonicity constants. Do this by imposing a restriction on the sum and withdrawing the term where $s = a$.

$$\begin{aligned} E_0 &= \omega_a\left(\mathrm{v}_a + \frac{1}{2}\right) + \chi_{aa}\left(\mathrm{v}_a + \frac{1}{2}\right)\left(\mathrm{v}_a + \frac{1}{2}\right) \\ &\quad + \sum_{s\neq a} \chi_{as}\left(\mathrm{v}_a + \frac{1}{2}\right)\left(\mathrm{v}_s + \frac{1}{2}\right) \\ &= \omega_a\left(0 + \frac{1}{2}\right) + \chi_{aa}\left(0 + \frac{1}{2}\right)\left(0 + \frac{1}{2}\right) \\ &\quad + \sum_{s\neq a} \chi_{as}\left(0 + \frac{1}{2}\right)\left(0 + \frac{1}{2}\right) \\ &= \frac{1}{2}\omega_a + \frac{1}{4}\chi_{aa} + \frac{1}{4}\sum_{s\neq a}\chi_{as} \end{aligned} \tag{27}$$

(ib) First excited state of normal coordinate a:

$$\begin{aligned} E_1 &= \omega_a\left(\mathrm{v}_a + \frac{1}{2}\right) + \chi_{aa}\left(\mathrm{v}_a + \frac{1}{2}\right)\left(\mathrm{v}_a + \frac{1}{2}\right) \\ &\quad + \sum_{s\neq a} \chi_{as}\left(\mathrm{v}_a + \frac{1}{2}\right)\left(\mathrm{v}_s + \frac{1}{2}\right) \\ &= \omega_a\left(1 + \frac{1}{2}\right) + \chi_{aa}\left(1 + \frac{1}{2}\right)\left(1 + \frac{1}{2}\right) \\ &\quad + \sum_{s\neq a} \chi_{as}\left(1 + \frac{1}{2}\right)\left(0 + \frac{1}{2}\right) \\ &= \frac{3}{2}\omega_a + \frac{9}{4}\chi_{aa} + \frac{3}{4}\sum_{s\neq a}\chi_{as} \end{aligned} \tag{28}$$

(ic) Fundamental frequency of normal coordinate a:

$$\begin{aligned} \nu_a &= E_1 - E_0 = \left(\frac{3}{2}\omega_a + \frac{9}{4}\chi_{aa} + \frac{3}{4}\sum_{s\neq a}\chi_{as}\right) \\ &\quad - \left(\frac{1}{2}\omega_a + \frac{1}{4}\chi_{aa} + \frac{1}{4}\sum_{s\neq a}\chi_{as}\right) \end{aligned}$$

$$\nu_a = \omega_a + 2\chi_{aa} + \frac{1}{2}\sum_{s\neq a}\chi_{as} \tag{29}$$

(iia) Vibrational ground state of normal coordinates b and c:

$$\begin{aligned} E_0 &= \omega_b\left(\mathrm{v}_b + \frac{1}{2}\right) + \omega_c\left(\mathrm{v}_c + \frac{1}{2}\right) + \sum_s \chi_{bs}\left(\mathrm{v}_b + \frac{1}{2}\right)\left(\mathrm{v}_s + \frac{1}{2}\right) \\ &\quad + \sum_s \chi_{cs}\left(\mathrm{v}_c + \frac{1}{2}\right)\left(\mathrm{v}_s + \frac{1}{2}\right) \end{aligned} \tag{30}$$

Now the outer sum runs over both normal coordinates. The sums can be restricted such that $s \neq b$ and $s \neq c$. Note that χ_{cb} does not appear in the original summations; however, the equivalent constant χ_{bc} does.

$$\begin{aligned} E_0 &= \omega_b\left(\mathrm{v}_b + \frac{1}{2}\right) + \omega_c\left(\mathrm{v}_c + \frac{1}{2}\right) + \chi_{bb}\left(\mathrm{v}_b + \frac{1}{2}\right)\left(\mathrm{v}_b + \frac{1}{2}\right) \\ &\quad + \chi_{cc}\left(\mathrm{v}_c + \frac{1}{2}\right)\left(\mathrm{v}_c + \frac{1}{2}\right) + \chi_{bc}\left(\mathrm{v}_b + \frac{1}{2}\right)\left(\mathrm{v}_c + \frac{1}{2}\right) \\ &\quad + \sum_{s\neq\{b,c\}} \chi_{bs}\left(\mathrm{v}_b + \frac{1}{2}\right)\left(\mathrm{v}_s + \frac{1}{2}\right) \\ &\quad + \sum_{s\neq\{b,c\}} \chi_{cs}\left(\mathrm{v}_c + \frac{1}{2}\right)\left(\mathrm{v}_s + \frac{1}{2}\right) \\ &= \omega_b\left(0 + \frac{1}{2}\right) + \omega_c\left(0 + \frac{1}{2}\right) + \chi_{bb}\left(0 + \frac{1}{2}\right)^2 \\ &\quad + \chi_{cc}\left(0 + \frac{1}{2}\right)^2 + \chi_{bc}\left(0 + \frac{1}{2}\right)^2 \\ &\quad + \sum_{s\neq\{b,c\}} \chi_{bs}\left(0 + \frac{1}{2}\right)^2 + \sum_{s\neq\{b,c\}} \chi_{cs}\left(0 + \frac{1}{2}\right)^2 \\ &= \frac{1}{2}\omega_b + \frac{1}{2}\omega_c + \frac{1}{4}\chi_{bb} + \frac{1}{4}\chi_{cc} + \frac{1}{4}\chi_{bc} \\ &\quad + \frac{1}{4}\sum_{s\neq\{b,c\}} (\chi_{bs} + \chi_{cs}) \end{aligned} \tag{31}$$

(iib) Doubly excited state in normal coordinates b and c (one quantum in each):

https://dx.doi.org/10.1021/acs.jpca.0c09526
J. Phys. Chem. A 2021, 125, 1301−1324

$$
\begin{aligned}
E_1 &= \omega_b\left(\mathrm{v}_b + \frac{1}{2}\right) + \omega_c\left(\mathrm{v}_c + \frac{1}{2}\right) + \chi_{bb}\left(\mathrm{v}_b + \frac{1}{2}\right)\left(\mathrm{v}_b + \frac{1}{2}\right) \\
&\quad + \chi_{cc}\left(\mathrm{v}_c + \frac{1}{2}\right)\left(\mathrm{v}_c + \frac{1}{2}\right) + \chi_{bc}\left(\mathrm{v}_b + \frac{1}{2}\right)\left(\mathrm{v}_c + \frac{1}{2}\right) \\
&\quad + \sum_{s\neq\{b,c\}} \chi_{bs}\left(\mathrm{v}_b + \frac{1}{2}\right)\left(\mathrm{v}_s + \frac{1}{2}\right) \\
&\quad + \sum_{s\neq\{b,c\}} \chi_{cs}\left(\mathrm{v}_c + \frac{1}{2}\right)\left(\mathrm{v}_s + \frac{1}{2}\right) \\
&= \omega_b\left(1 + \frac{1}{2}\right) + \omega_c\left(1 + \frac{1}{2}\right) + \chi_{bb}\left(1 + \frac{1}{2}\right)\left(1 + \frac{1}{2}\right) \\
&\quad + \chi_{cc}\left(1 + \frac{1}{2}\right)\left(1 + \frac{1}{2}\right) + \chi_{bc}\left(1 + \frac{1}{2}\right)\left(1 + \frac{1}{2}\right) \\
&\quad + \sum_{s\neq\{b,c\}} \chi_{bs}\left(1 + \frac{1}{2}\right)\left(0 + \frac{1}{2}\right) \\
&\quad + \sum_{s\neq\{b,c\}} \chi_{cs}\left(1 + \frac{1}{2}\right)\left(0 + \frac{1}{2}\right) \\
&= \frac{3}{2}\omega_b + \frac{3}{2}\omega_c + \frac{9}{4}\chi_{bb} + \frac{9}{4}\chi_{cc} + \frac{9}{4}\chi_{bc} \\
&\quad + \frac{3}{4}\sum_{s\neq\{b,c\}} (\chi_{bs} + \chi_{cs})
\end{aligned} \tag{32}
$$

(iic) Binary combination transition of normal coordinates b and c:

$$
\begin{aligned}
(\nu_b + \nu_c) &= E_1 - E_0 \\
&= \left(\frac{3}{2}\omega_b + \frac{3}{2}\omega_c + \frac{9}{4}\chi_{bb} + \frac{9}{4}\chi_{cc} + \frac{9}{4}\chi_{bc} + \frac{3}{4}\sum_{s\neq\{b,c\}} (\chi_{bs} + \chi_{cs})\right) \\
&\quad - \left(\frac{1}{2}\omega_b + \frac{1}{2}\omega_c + \frac{1}{4}\chi_{bb} + \frac{1}{4}\chi_{cc} + \frac{1}{4}\chi_{bc} + \frac{1}{4}\sum_{s\neq\{b,c\}} (\chi_{bs} + \chi_{cs})\right)
\end{aligned}
$$

$$
\begin{aligned}
(\nu_b + \nu_c) &= \omega_b + \omega_c + 2\chi_{bb} + 2\chi_{cc} + 2\chi_{bc} \\
&\quad + \frac{1}{2}\sum_{s\neq\{b,c\}} (\chi_{bs} + \chi_{cs})
\end{aligned} \tag{33}
$$

This can also be written in terms of one-quantum transitions of the normal modes:

$$
(\nu_b + \nu_c) = \nu_b + \nu_c + \chi_{bc} \tag{34}
$$

Likewise, for the first overtone of normal coordinate a. The frequency is given by

$$
2\nu_a = 2\omega_a + 6\chi_{aa} + \sum_{s\neq a} \chi_{as} \tag{35}
$$

Or expressed in terms of one-quantum transitions:

$$
2\nu_a = \nu_a + \nu_a + 2\chi_{aa} \tag{36}
$$

A simple formula for the VPT2 energy of any arbitrarily excited vibrational state can be determined in this manner. In the absence of anharmonic resonances, this is all that is required to obtain predictions of vibrational frequencies with VPT2.

2.5. Resonances in the Anharmonicity Constants. The anharmonicity constants contain "resonance denominators". These are terms in the summations that have differences of harmonic frequencies in their denominators. The resonance denominators shown below are those present in χ_{rr} and χ_{rs}, respectively.

$$
\frac{1}{2\omega_r - \omega_s} \tag{37}
$$

$$
\frac{1}{-\omega_r + \omega_s + \omega_t}, \qquad \frac{1}{\omega_r - \omega_s + \omega_t}, \qquad \frac{1}{\omega_r + \omega_s - \omega_t} \tag{38}
$$

For certain cases, it is clear that these terms will "blow up". This signifies a breakdown in the perturbation theory approximation. These terms can be selectively removed from the anharmonicity constant expressions. This is referred to as deperturbation. Deperturbation is as simple as subtracting the offending terms, undoing the damage caused by including them in the first place. The most commonly encountered cases are the Fermi resonances types I and II:

$$
\text{Type I: } \omega_a \approx 2\omega_b \qquad \text{Type II: } \omega_a \approx \omega_b + \omega_c
$$

From this point on, these same indices (a, b, and c) will be used whenever these resonance cases are referenced by name. Identification of resonances is somewhat arbitrary in nature, and many different resonance diagnostics have been used. The more successful ones typically weigh both the harmonic frequency difference and the magnitude of the associated cubic force constant. A Fermi resonance requires that vibrational states are sufficiently close in energy and are also coupled sufficiently strongly by the cubic terms in the potential expansion. A simple yet reliable resonance diagnostic is the eponymous Martin Test.[26] This is the difference between the variational and second-order perturbation corrections to the energies of a pair of states. The mathematical expressions are given below (eqs 39−42).

Perturbation Theory Correction (Type I):

$$
\frac{\left(\frac{1}{4}\phi_{abb}\right)^2}{\omega_a - 2\omega_b} \tag{39}
$$

Variational Correction (Type I) (obtained from eigenvalues of this matrix):

$$
\begin{aligned}
&\begin{pmatrix} \omega_a & \frac{1}{4}\phi_{abb} \\ \frac{1}{4}\phi_{abb} & 2\omega_b \end{pmatrix} \rightarrow \lambda \\
&= \frac{\omega_a + 2\omega_b \pm \sqrt{(\omega_a - 2\omega_b)^2 + \left(\frac{1}{4}\phi_{abb}\right)^2}}{2}
\end{aligned} \tag{40}
$$

Perturbation Theory Correction (Type II):

$$
\frac{\left(\frac{1}{2\sqrt{2}}\phi_{abc}\right)^2}{\omega_a - \omega_b - \omega_c} \tag{41}
$$

Variational Correction (Type II) (obtained from eigenvalues of this matrix):

$$
\begin{aligned}
&\begin{pmatrix} \omega_a & \frac{1}{2\sqrt{2}}\phi_{abc} \\ \frac{1}{2\sqrt{2}}\phi_{abc} & \omega_b + \omega_c \end{pmatrix} \rightarrow \lambda \\
&= \frac{\omega_a + \omega_b + \omega_c \pm \sqrt{(\omega_a - \omega_b - \omega_c)^2 + \left(\frac{1}{2}\phi_{abc}\right)^2}}{2}
\end{aligned} \tag{42}
$$

https://dx.doi.org/10.1021/acs.jpca.0c09526
J. Phys. Chem. A 2021, 125, 1301−1324

The difference can be evaluated for every two-state interaction, and a list of resonances can be populated by choosing an arbitrary cutoff value. A cutoff of 1 cm^{-1} is commonly used. The "harmonic derivatives" are an alternative resonance diagnostic, proposed by Matthews and Stanton and implemented in the GUINEA module of CFOUR 2.1.[27,28] These correspond to first and second derivatives of the VPT2 correction with respect to the harmonic frequencies.

After resonant terms are removed from an anharmonicity constant, it is customary to give the modified constant an asterisk and refer to it as "deperturbed". Moreover, any vibrational state calculated with deperturbed anharmonicity constants is also said to be deperturbed. To deperturb the anharmonicity constants for a Fermi Type I resonance, remove one term from χ_{bb} (eq 43) and one term from χ_{ab} (eq 44).

$$-\frac{1}{32}\left(\frac{\phi_{abb}^{\ 2}}{\omega_a - 2\omega_b}\right) \tag{43}$$

$$\frac{1}{8}\left(\frac{\phi_{abb}^{\ 2}}{\omega_a - 2\omega_b}\right) \tag{44}$$

To deperturb the anharmonicity constants for a Fermi Type II resonance, remove one term from both χ_{ab} and χ_{ab} (eq 45) and one term from χ_{bc} (eq 46).

$$\frac{1}{8}\left(\frac{\phi_{abc}^{\ 2}}{\omega_a - \omega_b - \omega_c}\right) \tag{45}$$

$$-\frac{1}{8}\left(\frac{\phi_{abc}^{\ 2}}{\omega_a - \omega_b - \omega_c}\right) \tag{46}$$

Quitting now and calculating vibrational energies with the deperturbed constants is sometimes called deperturbed second-order vibrational perturbation theory (DVPT2).[29] It provides an incomplete solution to the vibrational problem where the strongest couplings are not treated at all. This is not ideal. Instead, the strong couplings can be reintroduced within a variational framework. A small "effective Hamiltonian" matrix can be constructed of the vibrational states that are in resonance with each other. The diagonal elements of the matrix are taken to be the deperturbed VPT2 frequencies of each state. The off-diagonal elements are (typically) the same as what would be used for a standard variational calculation. The eigenvalues of such a matrix are the corrected vibrational energy levels, and the eigenvectors reflect the character/composition of the new vibrational states.

It is best to think about anharmonic coupling in terms of interacting *states* rather than interacting *transitions*; however, because all excited vibrational states share a common ground state, this choice has no bearing on the predicted transition frequencies. Choosing the diagonal elements of the matrix to be the energies of vibrational *states* and then subtracting from the ZPVE gives equivalent predictions to using the frequencies of *transitions* as the diagonal elements and defining the ZPVE as zero.

Software is available to perform these kinds of variationally corrected VPT2 calculations in a more (e.g., SPECTRO[30,31] and Gaussian's generalized second-order vibrational perturbation theory (GVPT2)[25,32] program) or less (e.g., CFOUR's GUINEA[27,33] program) automated manner. The applications discussed in this article focus on less automated approaches for the selection of resonances and interacting states; however, we acknowledge the value and appeal of black-box implementations of VPT.[25] At this point, it may also be useful to mention that the authors of this article are primarily practitioners of *ab initio* wave function theory. Much of what is suggested in this review (especially in section 2.7) comes from this perspective. We acknowledge several recent reviews of VPT application that instead describe the use of density functional theory (DFT) anharmonic force fields, which can also be effective and are typically obtainable at far lower computational cost.[6,34−36] Lastly, we briefly acknowledge an alternative method to variationally corrected VPT2, known as degeneracy-corrected VPT2 (DCVPT2) that handles resonance singularities in a different manner, eliminating the need for a variational step.[37] A method has recently been proposed by Barone and co-workers that smoothly mixes the DCVPT2 energy with the standard VPT2 energy, based on the proximity to resonance(s), in order to correct for the inaccuracy of DCVPT2 in certain cases that are far from resonance.[38]

2.6. Anharmonic Intensity. *2.6.1. Overview.* In order to understand transition intensity, it is useful to first introduce the language of mechanical anharmonicity and electrical anharmonicity.[39] Mechanical anharmonicity is sometimes also called intensity borrowing or intensity stealing. It describes the deviation from harmonicity (i.e., anharmonicity) of the vibrational wave functions. In contrast, electrical anharmonicity describes the deviation of the dipole moment function from linearity (in the normal coordinates). The approximation that the dipole moment is a linear function of the normal coordinates is referred to as the electrical harmonicity approximation. It is a special case of property anharmonicity, distinct from wave function anharmonicity. Various ways of evaluating intensity can be mechanically anharmonic, electrically anharmonic, both, or neither.[40]

Infrared intensity is proportional to the square of the transition dipole moment. It is most commonly expressed in units of kilometers per mole (km/mol) and less commonly as absorption cross-section (cm^2/molecule) or oscillator strength (unitless). The conversion factor to km/mol includes the frequency; the infrared intensity is therefore higher for higher-frequency transitions.[41] In this sense, one of the consequences of mechanical anharmonicity, which usually lowers frequencies, is a small reduction to intensities. For many applications, it is sufficient to determine only transitions from the vibrational ground state. However, in cases where low-energy states are thermally populated, transitions from excited states can be weighted by their Boltzmann populations. This can lead to issues if using VPT2 transition moments, as the available analytic expressions describe only transitions from the ground vibrational state.

After the transition dipole moment is determined, evaluation of infrared intensity is straightforward for full VPT2. For variationally corrected VPT2, detailed in section 3.1, the transition moments must first be transformed into the basis of the effective Hamiltonian eigenvectors. This allows transitions that are initially "dark" to obtain intensity via mechanical anharmonicity. This also means that variationally corrected VPT2 intensities are always at least partially mechanically anharmonic. The sum of the final intensities is usually close to, but not identical to, the intensity of the initial "bright" transition in the absence of the effective Hamiltonian treatment.

https://dx.doi.org/10.1021/acs.jpca.0c09526
J. Phys. Chem. A 2021, 125, 1301−1324

2.6.2. Evaluation of the Transition Dipole Moment. The dipole moment function may be expanded in the normal coordinates analogously to the potential energy (eq 2),

$$\hat{\mu}^{\alpha} = \mu_{\mathrm{eq}}^{\alpha} + \sum_{r} \mu_{r}^{\alpha} \hat{q}_{r} + \frac{1}{2} \sum_{rs} \mu_{rs}^{\alpha} \hat{q}_{r} \hat{q}_{s} + \frac{1}{6} \sum_{rst} \mu_{rst}^{\alpha} \hat{q}_{r} \hat{q}_{s} \hat{q}_{t} + \ldots \tag{47}$$

where μ_{eq} is the equilibrium dipole moment, μ_r, μ_{rs}, and μ_{rst} are first, second, and third dipole derivatives, respectively, and α indicates the inertial axis component. In practice, this expansion is usually also carried out such that the highest-order terms with no shared indices are neglected. Integrals of the dipole moment function, in the harmonic oscillator basis, can be evaluated with eqs 5−9. In this way, truncating eq 47 at the linear terms, harmonic intensities can easily be determined for transitions between arbitrary harmonic oscillator states.

It would appear that the most straightforward way to move beyond harmonic intensity would be to expand the dipole moment function further. For harmonic oscillators, contributions to the intensity follow an alternating pattern: one-quantum transition moments arise from the first, third, fifth, ... derivatives; two-quanta transition moments from second, fourth, sixth, ... derivatives; three-quanta transition moments from third, fifth, seventh, ... derivatives; etc. So, expanding the dipole moment function to the cubic terms provides the leading terms in the transition moments of one-, two-, and three-quanta transitions and the second term for one-quantum transitions. Determining transition moments using this expansion, in the harmonic oscillator basis, provides intensities that are electrically anharmonic but not necessarily mechanically anharmonic. Such a scheme is quite unusual, as it is uncommon to possess high-order dipole derivatives but not high-order potential derivatives, or it is uncommon to possess high-order potential derivatives and not use them in a treatment of mechanical anharmonicity. Moreover, the mechanical anharmonicity contribution to intensities is usually much more substantial than the electrical anharmonicity contribution.

As stated in section 2.6.1, intensities in variationally corrected VPT2 incorporate some mechanical anharmonicity effects (the most important ones, when the simulation is intelligently designed). For this reason, it is often adequate to use harmonic oscillator transition moments. These are simple to evaluate, resonance-free, and only require the first derivatives of the dipole moment. Yet it is important to appreciate that the basis functions for an effective Hamiltonian are not harmonic oscillator states; rather, they are partial VPT2 (or DVPT2) states. Therefore, the use of harmonic oscillator transition moments is not rigorously correct.

Transition moments may alternatively be evaluated in the framework of vibrational perturbation theory.[41−43] Transition moments at this level of approximation are both mechanically and electrically anharmonic. Transition moment integrals can be determined between any two VPT2 or VPT4 states, using a sum-over-states expression.[27,41,44] Analytic expressions for VPT2 transition moments also exist for one-, two-, and three-quanta transitions from the vibrational ground state.[29,41,43,45] The VPT2 transition moments for transitions of four quanta or greater are exactly zero. VPT2 transition moments are the most rigorous source of intensity for a VPT2 simulation. For variationally corrected VPT2, even the VPT2 transition moments are not fully rigorous, and it has been recognized that they require a form of deperturbation in order to correspond to the partial VPT2 effective Hamiltonian basis states.[46] Formulas for deperturbed transition moments of one- and two-quanta transitions (from the vibrational ground state) have been published by Vazquez and Stanton,[46] and GUINEA is capable of computing intensities for variationally corrected VPT2 for even more general cases.[27]

2.6.3. Corrected Analytic Expressions for VPT2 Transition Moments. This section reproduces equations from the literature for the VPT2 transition moments of one- and two-quantum transitions from the ground vibrational state. Furthermore, it corrects an error in the Coriolis contribution to the three-quantum transition moments that were presented recently.[47] It is self-evident that the Coriolis terms in the published $|ijk\rangle$ formula cannot be correct, as they lack i, j, k permutational symmetry. The $|iij\rangle$ Coriolis terms, as they were specialized from the $|ijk\rangle$ Coriolis terms, are also incorrect. However, Coriolis coupling makes no contribution to the transition moment for second overtones, $|iii\rangle$ The correctness of the new expression for the Coriolis contribution was confirmed by numerical comparisons with SoS computations.[41,48] They are presented in the Supporting Information (eqs S1−S5).

2.6.4. Resonances in VPT2 Transition Moments. In addition to being much more complicated than the corresponding energy expressions, VPT2 transition moments are susceptible to several kinds of anharmonic resonances.[46] The effect of resonances on transition moments can be profound, and because intensity is proportional to the square, the errors are magnified. Carefree use of VPT2 transition moments cannot therefore be recommended. Consider the cases of one-, two-, and three-quanta transitions from the vibrational ground state. The transition moment for two-quanta transitions is more compact than for the other two cases, and it contains only 1:2 resonance denominators (i.e., Fermi resonances). Identification of Fermi resonances via the Martin Test and subsequent deperturbation can be successful; however, a loose Martin Test threshold (perhaps 0.1 cm^{-1}) often performs better. The one- and three-quanta transition moments contain not only 1:2 resonance denominators but 1:1 and 1:3 Darling−Dennison resonances, respectively. While these types of resonances in transition moments are seldom as severe as Fermi resonances, they should not be ignored, and they must be identified using a different type of diagnostic. Similar to the way Fermi resonances are handled in Darling−Dennison constants (section 3.2), these 1:1 and 1:3 resonance terms are left deperturbed.

2.7. Computation of Anharmonic Force Fields.

2.7.1. Overview and Electronic Structure Considerations. When a vibrational spectrum is simulated via VPT2, the most time-consuming step is the computation of the anharmonic force field. This requires many derivatives of the electronic potential energy with respect to the normal coordinates. Anharmonicity constants require cubic force constants of the form ϕ_{rrr}, ϕ_{rrs}, and ϕ_{rst} (i.e., all of them); however, they only require the ϕ_{rrr} and ϕ_{rrss} quartic force constants. Therefore, in order to perform vibrational perturbation theory to second order, the complete sets of quadratic and cubic force constants and only a small part of the quartic force constants are required. The cubic and quartic force constants are commonly determined by numerically differentiating lower derivatives calculated at geometries displaced in the normal coordinates. The displacement algorithms provide enough derivative information to also compute the ϕ_{rrrs} and ϕ_{rrst} quartic force constants. The computation of quartic force fields truncated in this manner is

https://dx.doi.org/10.1021/acs.jpca.0c09526
J. Phys. Chem. A 2021, 125, 1301−1324

implemented in CFOUR, Gaussian, ORCA, and other packages.[27,32,49,50] It differs from a full quartic force field in that it lacks force constants with four distinct indices, ϕ_{rstu}. These would require many more displacements and derivative calculations. In VPT2+K (section 3.2), the lack of ϕ_{rstu} force constants means that certain resonance constants cannot be determined.

In choosing a level of theory at which to compute force constants, it is most important to consider the reference wave function, the basis set, and the level of electron correlation. With regard to the reference wave function, the first question that must be answered is whether a single-configurational description is a reasonable starting point or if the wave function is intrinsically multiconfigurational in nature. When this is in doubt, the multiconfigurational character of a system can be judged by performing complete active space self consistent field (CASSCF) computations.[51,52] When affordable, the active space is chosen as the valence space, but this can be truncated to remove strongly doubly occupied orbitals or nearly unoccupied orbitals. At least a polarized double-ζ basis set should be used. If more than one of the squared CASCI coefficients adopts a large value, then this is indicative of a multiconfigurational system. The cutoff value is arbitrary; however, a value of 0.05 or higher for the second most dominant configuration is considered to be notable, and a value of 0.10 or higher is considered to be severe. Single-reference coupled cluster (CC) computations also have diagnostic value, as the T_1 and T_2 amplitudes reflect the importance of mixing with excited configurations. A large T_2 amplitude can indicate that the wave function has biradical character.[53] Large T_1 amplitudes are more difficult to interpret. In some open-shell systems, large T_1 amplitudes are not a cause for concern; instead, they are reflective of orbital relaxation effects.[54]

Once it is established that a system is single-configurational, the starting point for describing the electronic wave function is the Hartree−Fock self-consistent field (HF-SCF) method. Closed shell systems are described from a restricted Hartree−Fock (RHF) starting point, which usually does not warrant any special discussion. Unrestricted Hartree−Fock (UHF) and restricted open shell Hartree−Fock (ROHF) are the two most commonly encountered references for open shell systems, and post-HF electron correlation methods and analytic derivatives based upon both types are available. The correct choice is not at all obvious.[55,56] A UHF reference is susceptible to a phenomenon known as spin contamination wherein the wave function is artificially stabilized by mixing with wave functions of different multiplicities. As a consequence of this, the UHF wave function is not an eigenfunction of the total spin squared operator; however, the true wave function must be. Electron correlation repairs this; particularly, iterative coupled cluster methods are very effective at reducing the spin contamination of the wave function. ROHF does not suffer from spin contamination, and on this basis it would seem to be the superior choice to UHF. However, it is interesting to note that typical electron correlation treatments based on an ROHF reference can actually introduce small amounts of spin contamination.[57,58]

There is a further problem called artifactual symmetry breaking. This can affect both types of reference; however, it has been stated that ROHF is more susceptible.[55] Artifactual symmetry-breaking can occur when an alternative, lower-energy SCF solution exists, which has lower symmetry than the point group of the system. Such a thing is also not physical, as the wave function symmetry must match the molecular symmetry. Stated differently, the molecular orbitals must transform as irreducible representations of the point group of the molecule. At higher-symmetry structures, it is sometimes possible to constrain the wave function to conform to the molecular symmetry. However, it is much more difficult to prevent the SCF procedure from converging to a broken symmetry solution at a displaced, lower-symmetry geometry, where the real and artifactual solutions have the same symmetry. Numerically differentiating points that have converged to different SCF solutions will lead to nothing but garbage. In this way, symmetry-breaking can be a serious concern whenever numerical differentiation is employed, such as in the determination of quartic force fields. Symmetry breaking is not totally unrelated to spin contamination; oftentimes, the alternative SCF solutions can be identified by their expectation values of the total spin squared operator. Finally, it is important to understand that symmetry breaking does not actually require there to be any symmetry elements. The essence of artifactual symmetry breaking is the incorrect localization of electron density; this can happen even in the absence of symmetry, and spurious SCF solutions will arise.

There is a third, even less obvious source of error that can affect both UHF and ROHF references. In certain regions of nuclear displacement space, different SCF solutions may become exactly degenerate; however, the true wave functions are unlikely to be. The different SCF solutions may correspond to real, excited electronic states, or they may be spurious, localized solutions, like those discussed above. These are referred to as orbital instabilities.[59,60] Properties that depend upon derivatives of the electronic wave function (e.g., force constants) will tend toward positive or negative infinity as the points of degeneracy are approached. Such behavior would be reasonable if these were the true wave functions of two electronic states in the vicinity of an intersection. Unfortunately, the degeneracies between SCF solutions are still meaningful, even in highly correlated wave functions. When the equilibrium geometry determined with a correlated level of theory is near the location of an SCF degeneracy, the accuracy of force constant predictions is degraded. More complete electron correlation reduces the size of these problematic "near instability" regions, in nuclear configuration space, and iterative methods are more effective. In fact, perturbative methods can actually worsen the problem.[59] Orbital instabilities are only completely eliminated in the full CI limit. It is effectively a matter of luck as to what extent vibrational frequencies are affected by near-instabilities. A useful diagnostic for this problem is the "stability analysis" implemented in most software packages, which evaluates the second derivatives of the HF-SCF energy with respect to rotations (i.e., optimizations) of the orbitals. Small second derivatives (either positive or negative valued) may be a cause for concern.[61]

It is for these reasons that it is advisible to perform computations on open-shell systems with both types of reference and to compare the frequencies. If they match closely, it is unlikely that any of these reference problems are an issue. If they disagree, then more detailed investigations should be carried out, potentially involving EOM-CC, Brückner CC, or multireference methods.[62−64] Higher-order coupled cluster methods can offer more of a brute force solution, particularly the iterative methods such as CCSDT, which are more robust in the vicinity of wave function instabilities.

The most affordable treatment of dynamical electron correlation is by Møller−Plesset second-order perturbation

https://dx.doi.org/10.1021/acs.jpca.0c09526
J. Phys. Chem. A 2021, 125, 1301−1324

theory (MP2), and it is fairly accurate for making force constant predictions. In order to achieve a description of harmonic frequencies superior to that of MP2, CCSD(T) should typically be chosen next. Frequencies from CCSD are often worse than MP2, except in cases where the electronic structure is particularly challenging or pathological.[65] Other electronic structure methods, such as EOM-CC, are normally reserved for troublesome systems. EOM-CC can also be an excellent choice for describing open-shell singlets or excited states, rivaling or surpassing multireference perturbation theory. When extreme accuracy is the goal, it may be desirable to extend electron correlation to CCSDT(Q) for a well-behaved system. Usually, this should also be balanced with various auxiliary corrections such as core-correlation, scalar relativity, the diagonal Born−Oppenheimer correction, and spin−orbit coupling, as in various high-accuracy thermochemistry methodologies.[66,67] These methodologies often utilize explicit correlation or extrapolation techniques to approach a complete basis set (CBS) limit quality description.[68−70]

Refocusing the discussion away from composite model chemistries and back to single "levels of theory", the basis sets of choice for computing vibrational frequencies of small organic molecules are often derived from the atomic natural orbital (ANO) basis set of Almlöf and Taylor.[71] Two benchmarking studies have found that the ANO basis sets generally perform well for harmonic frequencies, and they often perform better than the similar sized Dunning basis sets.[72,73] Their superior performance is more pronounced for smaller basis sets (double and triple-ζ) quality. The full ANO basis set is quadruple-ζ, denoted ANO2, and its triple and double-ζ truncations are denoted ANO1 and ANO0, respectively. Section 2.7.2 delves into more detail about effective use of these basis sets.

A final consideration in choosing an electronic structure method is the availability of analytic energy derivatives. Analytic formulations of third and fourth derivatives are only available for Hartree−Fock[74−76] and DFT[77] and are not commonly implemented in quantum chemistry software packages. A quartic force field contains up to fourth geometrical derivatives of the electronic energy; thus, quartic force fields are usually determined numerically. Differentiation of lower analytic derivatives (i.e., first or second) helps to reduce the number of normal coordinate displacements and reduce the numerical differentiation error. Electronic structure methods with at least analytic first derivatives available are very desirable for computation of quartic force fields. The CFOUR package has analytic derivatives implemented for numerous *ab initio* methods.[33] A few important methods are listed below. Hartree−Fock (RHF, UHF, and ROHF) has up to second derivatives. Most correlated methods based on ROHF [MP2, CCSD, CCSD(T)] have first derivatives, and most correlated methods based on RHF and UHF [MP2, CCSD, CCSD(T)] have up to second derivatives.[78,79] For higher-level methods, CCSDT, CCSDT(Q), and CCSDTQ first derivatives are available with RHF.[33,80] First derivatives are also available with various EOM-CC models. Access to analytic second derivatives for higher-order standard coupled cluster methods is possible with the MRCC program.[81,82]

2.7.2. Hybrid Force Field Approximations. The motivation behind making a "hybrid approximation" to a quartic force field will be introduced first, and then it will actually be explained what is meant by the term. The use of hybrid approximations is motivated by three points. First, harmonic frequencies are more sensitive to the level of theory than higher-order force constants. A primary reason for this is the increased importance of the nuclear repulsion energy for higher-order derivatives, which is always treated exactly.[83,84] Second, it is intuitively obvious that it requires less computational expense to compute harmonic frequencies than to compute an entire quartic force field at the same level of theory. Third, anharmonic predictions are more sensitive to the quality of the harmonic frequencies, as these constitute the zeroth-order picture, than they are to the quality of the higher-order force constants.

A hybrid approximation entails the combination of force constants from different levels of theory, ideally forming a force field that is both accurate and economical. For the work discussed herein, harmonic (i.e., quadratic) force constants are evaluated at a "higher-level" of theory, and the cubic/quartic force constants are evaluated at a "lower-level" of theory. There are several approaches to combining force constants. The approaches can be classified on the basis of whether they make the following two assumptions: (i) The anharmonic coupling is well described at the lower-level of theory. (ii) The normal coordinates are the same at both levels of theory. Both assumptions are generally valid, if very high levels of theory can be applied to both the harmonic and anharmonic parts of the force field. If this is the case, then details of how the hybrid approximation is applied are unimportant. In the unsaturated hydrocarbon examples of sections 3.1.1 and 3.8.2, the higher and lower levels of theory are CCSD(T)/ANO1 and CCSD(T)/ANO0, respectively, and the combination of both into a hybrid force field will be indicated as CCSD(T)/ANO[1,0]. The effectiveness of hybrid approximations has been evaluated by Polik and co-workers in a recent review of VPT2+K application.[85]

The first approach, denoted "additive", makes both assumptions. The VPT2 equations are solved with the nonhybrid (i.e., pure), lower-level quartic force field, and additive anharmonic corrections are determined. These are simply the difference between the VPT2 frequency and the harmonic frequency. The corrections are then applied to the higher-level harmonic frequencies. The earliest application of the additive hybrid approximation appears to have been made by Handy and co-workers in a 1989 study on hydrogen peroxide.[86] This approach is not generally recommended, as the first assumption is particularly poor when dealing with CH stretches. In this spectral region, the most important couplings occur between singly excited CH stretches and doubly excited HCH bends; however, the basis set requirements are much greater for CH stretches than for HCH bends. If the Fermi coupling problem is solved in a small one-electron basis set (e.g., using CCSD(T)/ANO0), the CH stretching harmonic frequencies will be systematically too high (10−20 cm^{-1} or more), but the HCH bending harmonic frequencies will be fairly well converged. The stretch−bend coupling will not be accurately described; its strength is typically underestimated. A further concern arises with additive anharmonicity corrections derived from effective Hamiltonian treatments. Since the final states can be of significantly mixed character, but the corrections are applied to pure, harmonic states, the additive approach can be unsatisfying.

The second approach is denoted "substituted", and it makes only the second assumption.[87] The lower-level harmonic force constants are first replaced with their higher-level analogues, in the quartic force field. Then the VPT2 equations are solved with the modified force field. This approach is generally recommended, as it has no additional cost, and the two problems

https://dx.doi.org/10.1021/acs.jpca.0c09526
J. Phys. Chem. A 2021, 125, 1301−1324

discussed with the additive approach are completely overcome. The substituted approach allows for more natural effective Hamiltonian treatments. However, the second assumption may still cause problems for larger, lower-symmetry systems, where the localized vs delocalized nature of the normal coordinates becomes more sensitive to the level of theory.

The third approach, denoted "transformed", discards the second assumption, eliminating error due to differences in the normal coordinates.[88,89] A type of transformed hybrid approximation used recently by the authors transforms lower-level cubic/quartic force constants into higher-level normal coordinates (corresponding to the quadratic force constants).[88] This implies that the harmonic force constants have also been substituted as in the second approach. The disadvantage of the transformed approach is that it requires a full quartic force field, which includes the seldom-computed force constants with four distinct indices. The computation of a full quartic force field can be several times more expensive; however, it can still be less expensive than using the higher level of theory for all force constants. Full quartic force fields are, however, highly desirable for simulations of multiple isotopologues, as the force field of one isotopologue may be freely transformed into the normal coordinates of any other isotopologue (even those of lower point group symmetry).

A fourth approach has been applied to acetonitrile and other systems by Pouchan and co-workers.[90−92] This entails first the determination of CCSD(T) harmonic frequencies and normal coordinates and then the direct evaluation of cubic and quartic force constants, in those normal coordinates, at a lower level of theory. In their work, their lower level of theory involves DFT. In their applications, DFT exhibits satisfactory accuracy for cubic and quartic force constants. This direct approach does not require a full quartic force field; however, it introduces errors because the DFT force constants are evaluated at a nonstationary geometry (i.e., the first derivatives of the potential energy are not zero). Solutions to this problem have been discussed in great detail; however, the magnitude of the errors has not been well studied.[83,84]

3. RESULTS AND DISCUSSION

3.1. Illustrative Examples. This section introduces the first two example systems, using them to illustrate some of the considerations involved in performing VPT simulations. This sets a precedent for the structure of the remainder of this article; further aspects of VPT2 simulations are discussed with reference to these examples and others. For instance, the formaldehyde example in section 3.1.2 motivates the introduction of the Darling−Dennison resonance constants in section 3.2, seeing VPT2 extended fully to VPT2+K.

3.1.1. Simulation of the CH Stretches of Cyclopentadiene. Cyclopentadiene is an 11-atom system ($3N - 6 = 27$ normal modes) with C_{2v} symmetry. In a semirigid system like this, the CH stretch transitions are often the most anharmonic and therefore the most interesting to model. Vibrational states with one quantum of CH stretch excitation frequently fall close in energy to states with two quanta of CH bending and/or C=C stretching excitation. When those stretching and bending normal modes primarily involve motion of the same atoms, the force constants can also be quite large. The procedure for predicting the infrared spectrum is divided into six steps.

Step 1: Compute the anharmonic force field. This example uses a hybrid quartic force field. In this force field, the quadratic force constants are computed at the CCSD(T)/ANO1 level of theory, and the cubic and quartic force constants are computed at the CCSD(T)/ANO0 level of theory (a smaller basis set). The substituted hybrid scheme is employed. This force field contains 990 unique cubic force constants and 2548 unique quartic force constants (of which 368 are sufficient for VPT2). The C_{2v} symmetry of the system is taken into account during the calculation, so many force constants are rigorously zero. This has significantly reduced the size of the force field.

Step 2: Calculate the anharmonicity constants. The full VPT2 spectrum of the CH stretching fundamentals is shown in Figure 1. Harmonic oscillator intensity is used, on the basis of a linear expansion of the transition dipole moment. This choice is likely not the most accurate option, but it avoids overcomplicating the discussion. Something is so wrong that an axis break is necessary. Frequency predictions that are hundreds or thousands of wavenumbers outside of the normal range, such as the 4700 cm^{-1} CH stretching fundamental here, usually indicate an untreated Fermi resonance. Now it should be considered whether Fermi resonances are active.

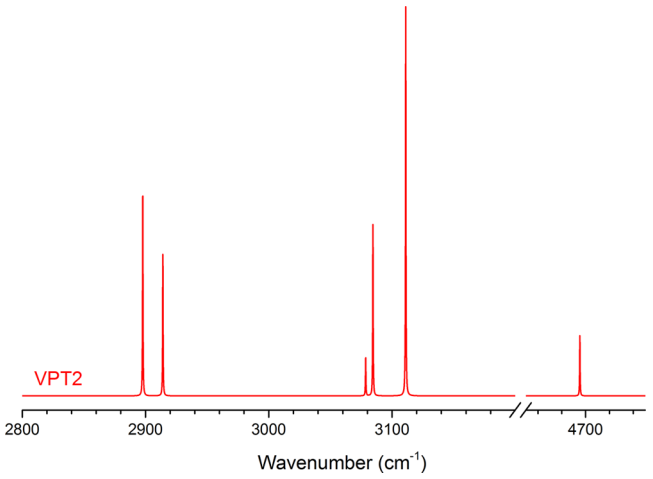

Figure 1. Full VPT2 simulation of the CH stretching fundamentals of cyclopentadiene. The quartic force field was determined using the CCSD(T)/ANO[1,0] hybrid model.

Step 3: Establish a list of resonances. This should reveal why there is a CH stretch fundamental at 4700 cm^{-1}. Using the Martin Test with a 1 cm^{-1} threshold, which is typical, four Fermi resonances are identified: three Type I and one Type II (Table 1). Refer to the list of normal coordinates to decide which resonances are relevant for the CH stretching region (Table 2). Four are linear combinations of the CH stretches on the ring, and the other two correspond to the symmetric and antisymmetric stretches of the CH_2 group. Inspecting the resonance list, note that the first two do not affect the CH stretches. They manifest in anharmonicity constants that are not

Table 1. Fermi Resonances in Cyclopentadiene[a]

resonance	Γ	energy separation	cubic force constant	variational − perturbational
$\omega_8 \approx 2\omega_{14}$	A_1	10.9	−31.6	1.6
$\omega_6 \approx 2\omega_{13}$	A_1	2.4	−11.2	1.4
$\omega_{20} \approx \omega_4 + \omega_{22}$	B_2	64.6	−89.7	2.6
$\omega_1 \approx 2\omega_{22}$	A_1	0.3	88.1	1567.2

[a]All quantities are given in wavenumbers. Resonances were identified with a 1 cm^{-1} threshold Martin Test, shown in the last column.

https://dx.doi.org/10.1021/acs.jpca.0c09526
J. Phys. Chem. A 2021, 125, 1301−1324

Table 2. Normal Coordinates of Cyclopentadiene[a]

no.	Γ	description	no.	Γ	description	no.	Γ	description
1	A_1	$\nu_s^{in}(CH)$	10	A_1	δ_s(ring)	19	B_1	ring puckering
2	A_1	$\nu_{as}^{in}(CH)$	11	A_2	$\tau(CH_2)$	20	B_2	$\nu_s^{out}(CH)$
3	A_1	$\nu_s(CH_2)$	12	A_2	$\rho_{w,as}^{out}(CH)$	21	B_2	$\nu_{as}^{out}(CH)$
4	A_1	ν_s(C═C)	13	A_2	$\rho_{w,s}^{out}(CH)$	22	B_2	ν_{as}(C═C)
5	A_1	$\delta_{as}^{in}(CH)$	14	A_2	τ(ring)	23	B_2	$\delta_{as}^{out}(CH)$
6	A_1	$\delta(CH_2)$	15	B_1	$\nu_{as}(CH_2)$	24	B_2	$\rho_w(CH_2)$
7	A_1	$\delta_s^{in}(CH)$	16	B_1	$\rho_{w,as}^{in}(CH)$	25	B_2	$\delta_s^{out}(CH)$
8	A_1	ν(C—C)	17	B_1	$\rho_r(CH_2)$	26	B_2	ν_{as}(C—C—C)
9	A_1	ν_s(C—C—C)	18	B_1	$\rho_{w,s}^{in}(CH)$	27	B_2	δ_{as}(ring)

[a]Modes are ordered in the standard spectroscopic convention. Symmetries and qualitative descriptions are given.

present in the energy expressions for the CH stretch fundamentals. As long as only CH stretch transitions are desired, these resonances can be ignored. The last two resonances directly involve CH stretches. The highest-frequency CH stretch states are strongly coupled to doubly excited C═C stretching states. The first resonance occurs between B_2 states and the second between A_1 states.

Step 4: Deperturb the anharmonicity constants accordingly. The consequences of deperturbing the anharmonicity constants for the B_2 resonance are shown below.

$$\chi_{4,20} = 15.3 \rightarrow \chi_{4,20}^{*} = -0.3,$$
$$\chi_{20,22} = 15.6 \rightarrow \chi_{20,22}^{*} = 0.0,$$
$$\chi_{4,22} = -32.2 \rightarrow \chi_{4,22}^{*} = -16.7$$

Deperturbing the anharmonicity constants for the A_1 resonance has the following effects.

$$\chi_{22,22} = -798.3 \rightarrow \chi_{22,22}^{*} = -3.7,$$
$$\chi_{1,22} = 3177.1 \rightarrow \chi_{1,22}^{*} = -1.1$$

Step 5: Treat the resonances. This anharmonic coupling problem is quite simple, and it requires only two 2 × 2 effective Hamiltonians. The solutions of matrix eigenvalue problems will be presented in a form that simplifies their interpretation. The rows of the eigensolution represent the "unmixed" DVPT2 basis functions, in the same order as they were arranged in the effective Hamiltonian. Each column corresponds to a final vibrational state, headed by its eigenvalue. The numbers within the matrix are the squared eigenvector coefficients. They are interpreted as the fraction of each original DVPT2 vibrational state that is present in the final states. Variational treatment of the B_2 symmetry resonance is detailed below (eqs 48−50).

$$H_{\text{eff}} = \begin{pmatrix} \nu_{20}^{*} & \frac{1}{2\sqrt{2}}\phi_{20,4,22} \\ \frac{1}{2\sqrt{2}}\phi_{20,4,22} & (\nu_4 + \nu_{22})^{*} \end{pmatrix} \tag{48}$$

$$H_{\text{eff}} = \begin{pmatrix} 3095.5 & -31.7 \\ -31.7 & 3068.0 \end{pmatrix} \tag{49}$$

$$\begin{bmatrix} & \mathbf{3116.3} & \mathbf{3047.2} \\ |\nu_{20}\rangle & 0.70 & 0.30 \\ |\nu_4 + \nu_{22}\rangle & 0.30 & 0.70 \end{bmatrix} \tag{50}$$

As a result of the B_2 resonance, the fundamental is pushed up, and the combination is pushed down in frequency by 21 wavenumbers (eq 50). The states mix considerably, but the transition at 3116.3 cm^{-1} is best described as a CH stretch fundamental, and the transition at 3047.2 cm^{-1} is primarily the symmetric + antisymmetric C═C stretch combination. Treatment of the A_1 resonance proceeds similarly (eqs 51−53).

$$H_{\text{eff}} = \begin{pmatrix} \nu_1^{*} & \frac{1}{4}\phi_{1,22,22} \\ \frac{1}{4}\phi_{1,22,22} & 2\nu_{22}^{*} \end{pmatrix} \tag{51}$$

$$H_{\text{eff}} = \begin{pmatrix} 3106.1 & 22.0 \\ 22.0 & 3152.0 \end{pmatrix} \tag{52}$$

$$\begin{bmatrix} & \mathbf{3160.8} & \mathbf{3097.2} \\ |\nu_1\rangle & 0.14 & 0.86 \\ |2\nu_{22}\rangle & 0.86 & 0.14 \end{bmatrix} \tag{53}$$

The overtone is pushed up, and the fundamental is pushed down in frequency by 9 cm^{-1}. They mix more weakly than the B_2 states, so the transitions are still well described as a CH stretch fundamental at 3097.2 cm^{-1} and the first overtone of the antisymmetric C═C stretch at 3160.8 cm^{-1}.

These results illustrate that the variational − perturbational difference from the Martin Test is not always reflective of how strong the mixing will be, as it is based upon a two-state interaction of zeroth-order harmonic oscillator states, whereas the final mixing occurs after the diagonal elements have been "dressed" to account for weak interactions with other states. Note also that the A_1 resonance is predicted to be so strong because the zeroth-order states are less than 1 cm^{-1} apart. The harmonic frequencies of these states are not fully converged, and they might change by 10 cm^{-1} or more if they are computed with more complete basis sets. Small changes could lead to a much smaller value of the resonance diagnostic.

Step 6: Simulate the spectrum. As with the full VPT2 spectrum, harmonic intensity is used. In the case of resonant interactions, the harmonic intensity can be distributed proportional to the state mixing. For example, the B_2 effective Hamiltonian gives transitions at 3047.2 and 3116.3 cm^{-1}. The lower-frequency transition, $\nu_4 + \nu_{22}$, steals 30% of the intensity from ν_{20}, which is left with 70%. In this model, mixing is necessary to confer intensity to combinations and overtones.

Figure 2 shows the variationally corrected simulation. This type of simulation has occasionally been called VPT2+F, where the F indicates some explicit treatment of Fermi coupling.[87] It

https://dx.doi.org/10.1021/acs.jpca.0c09526
J. Phys. Chem. A 2021, 125, 1301−1324

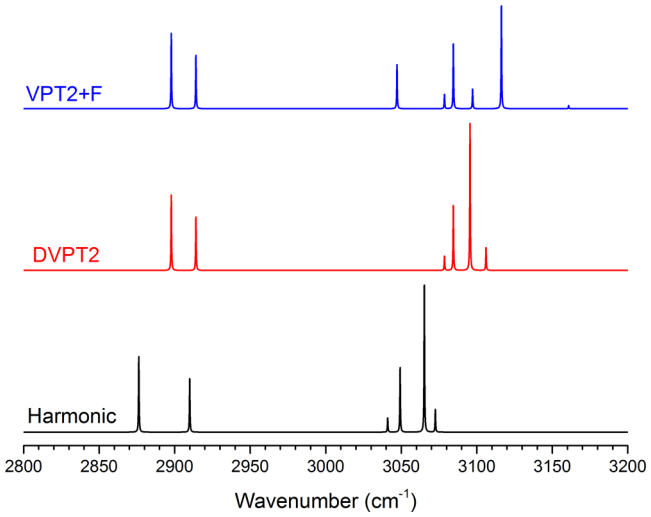

Figure 2. Various anharmonic simulations of the cyclopentadiene CH stretching region.

would be interesting to see how this simulation compares to a scaled harmonic spectrum, which is a far simpler and cheaper alternative. The scaling factor for the harmonic spectrum is chosen to best reproduce the experimental band origins of the two nonresonant fundamentals centered around 2900 cm^{-1}. Additionally, a DVPT2 simulation in included in the comparison (Figure 2).

The structures of the harmonic and DVPT2 spectra are very similar. They each have only six transitions because we have provided no mechanism for dark states to borrow intensity. The effective Hamiltonian procedure from VPT2+F simultaneously corrects the frequencies of the fundamentals and the strongly coupled two-quanta states and also lights up the dark two-quanta transitions, giving intensity predictions that are usually qualitatively correct. Observe that the combination transition at 3047 cm^{-1} is actually more intense than some of the fundamentals.

The theoretical transitions are now compared to experimental values. The experimental frequencies come from a series of gas- and liquid-phase studies conducted at room temperature. Band origins derived from these measurements are not highly accurate (~10 cm^{-1} uncertainty). For some transitions, their symmetries could be experimentally deduced on the basis of Raman depolarization ratios and gas-phase rotational contours. This is especially useful for assigning the transitions above 3000 cm^{-1}, which are somewhat dense but can be distinguished as being either A_1 or B_2 symmetry.

The lowest-frequency transitions are the A_1 and B_1 symmetry CH_2 stretches. They have been observed as two medium-strength bands at 2886 and 2900 cm^{-1}, respectively. Nothing else is observed in the vicinity of these. The simulation places these in the correct order, at 2905 and 2914 cm^{-1}. In this spectral region, VPT2+F offers no advantage over VPT2, and even an assignment based upon harmonic frequencies will be successful. On the high-frequency side, the first overtone of the antisymmetric C═C stretch was assigned as a weak feature at 3161 cm^{-1}. The VPT2+F simulation also places it at 3161 cm^{-1}. Two medium-strength A_1 transitions were observed at 3091 and 3075 cm^{-1} and were assigned to the fundamentals. The lower transition from the A_1 effective Hamiltonian is predicted at 3097 cm^{-1}. This is a good candidate for the higher-frequency transition. The 3075 cm^{-1} transition probably corresponds to the in-phase antisymmetric CH stretch fundamental, predicted at 3084 cm^{-1}.

One medium-strength B_2 band was observed at 3105 cm^{-1} and assigned to the symmetric out-of-phase CH stretch. This same transition is predicted at 3116 cm^{-1} from diagonalization of the effective Hamiltonian. The other transition that is predicted from the B_2 effective Hamiltonian is the combination band at 3047 cm^{-1}. This matches well with another medium-strength experimental band found at 3043 cm^{-1}. This feature was previously assigned to the other B_2 fundamental; however, assignment to the combination band is also consistent with the symmetry. Of the methods compared, only VPT2+F predicts intense transitions in the vicinity of both experimental bands. It is plausible that the remaining B_2 fundamental was too weak to observe and/or obscured by other spectral features. VPT2 predicts that it occurs at 3079 cm^{-1} and that it is the least intense of all the fundamentals.

Several more transitions have been observed in this spectral region. For example, the first overtone of the symmetric C═C stretch was assigned as a weak feature at 2994 cm^{-1}. Since no resonances are associated with it, full VPT2 should provide a reasonable description. It places it at 2996 cm^{-1}, showing excellent agreement. In the remainder of this article, further example problems are discussed for several small molecules (ethylene, formaldehyde, and water). These systems exhibit more complicated resonance interactions.

3.1.2. Out-of-Phase Symmetric CH_2 Stretch of Ethylene. The anharmonic coupling in ethylene was the subject of a 1995 paper by J. M. L. Martin et al.[26] This was the same study that proposed the Martin Test for Fermi resonances. In their work, they discuss a resonance triad involving ν_{11}, $\nu_2 + \nu_{12}$, and $2\nu_{10} + \nu_{12}$. These states are the out-of-phase symmetric CH_2 stretch fundamental, [C═C stretch + out-of-phase CH_2 scissor], and [2(in-phase CH_2 rock) + out-of-phase CH_2 scissor], respectively. The smallest effective Hamiltonian that can describe their interaction will be a 3 × 3. When more than two vibrational states are mutually coupled in an effective Hamiltonian, this is referred to as a resonance polyad. Ethylene will be described using a CCSD(T)/cc-pVTZ force field, the same level of theory used by Martin. This quartic force field contains only 60 unique cubic and 115 unique quartic force constants. This time, the procedure will begin with computation of the Martin Diagnostics for all two-state interactions (Table 3).

Table 3. Fermi Resonances in Ethylene[a]

resonance	Γ	energy separation	cubic force constant	variational − perturbational
$\omega_{11} \approx \omega_2 + \omega_{12}$	B_{3u}	11.7	125.7	130.2
$\omega_2 \approx 2\omega_{10}$	B_{3u}	25.7	−53.0	1.2

[a]All quantities are given in wavenumbers. Resonances were identified with a 1 cm^{-1} threshold Martin Test, shown in the last column.

With a cutoff value of 1 cm^{-1}, two resonances are identified. These are the same resonances that give rise to the polyad discussed by Martin. It may not be immediately obvious why this is the case. The first resonance directly involves the CH stretch fundamental. In isolation, it could be treated by diagonalizing the 2 × 2 matrix of ν_{11}^* and $(\nu_2 + \nu_{12})^*$. However, the anharmonicity constants will have been deperturbed for the second resonance as well. This deperturbs $\nu_2 + \nu_{12}$ for an additional interaction: with $2\nu_{10} + \nu_{12}$. This state also must be included in the effective

https://dx.doi.org/10.1021/acs.jpca.0c09526
J. Phys. Chem. A 2021, 125, 1301−1324

Hamiltonian in order for the treatment of the coupling to be complete.

To understand the origin of the three-quanta state above, it may also be helpful to recall that, in VPT2, the vibrational energies of multiply excited states can be expressed as a sum of energies of singly excited states and certain anharmonicity constants. When ν_2 is deperturbed for its interaction with $2\nu_{12}$, the analogous interaction between $\nu_2 + \nu_{12}$ and $2\nu_{10} + \nu_{12}$ is also deperturbed, or more generally all interactions between the states: $\nu_2 + \nu_n$ and $2\nu_{10} + \nu_n$. When multiple resonances are connected to each other in this way, the complexity of the effective Hamiltonian can increase significantly. This phenomenon of "connected" resonances is discussed further in section 3.7. Now calculate the anharmonicity constants and deperturb for these two resonances. The effect of the $\omega_{11} \approx \omega_2 + \omega_{12}$ resonance is shown below.

$$\chi_{2,11} = -177.4 \rightarrow \chi^*_{2,11} = -8.2,$$
$$\chi_{11,12} = -182.3 \rightarrow \chi^*_{11,12} = -13.1,$$
$$\chi_{2,12} = 166.1 \rightarrow \chi^*_{2,12} = -3.0$$

The effect of the $\omega_2 \approx 2\omega_{10}$ resonance is shown below.

$$\chi_{2,2} = 1.2 \rightarrow \chi^*_{2,2} = 4.6, \qquad \chi_{2,10} = 5.9 \rightarrow \chi^*_{2,10} = -7.8$$

Resonance treatment is shown below (eqs 54−56). This resonance polyad might be described as $\nu_2 + \nu_{12}$ simultaneously participating in a Fermi Type II interaction with ν_{11} and a Fermi Type I interaction with $2\nu_{10} + \nu_{12}$. State mixing is extensive; however, the transition at 2978.4 cm^{-1} arguably remains pure enough to be called the CH stretch fundamental (eq 56).

$$H_{\text{eff}} = \begin{pmatrix} \nu^*_{11} & \frac{1}{2\sqrt{2}}\phi_{2,11,12} & \approx 0 \\ \frac{1}{2\sqrt{2}}\phi_{2,11,12} & (\nu_2 + \nu_{12})^* & \frac{1}{4}\phi_{2,10,10} \\ \approx 0 & \frac{1}{4}\phi_{2,10,10} & (2\nu_{10} + \nu_{12})^* \end{pmatrix} \tag{54}$$

$$H_{\text{eff}} = \begin{pmatrix} 3001.8 & 44.4 & 0 \\ 44.4 & 3064.6 & -13.3 \\ 0 & -13.3 & 3085.4 \end{pmatrix} \tag{55}$$

$$\begin{bmatrix} & \mathbf{3098.5} & \mathbf{3074.9} & \mathbf{2978.4} \\ |\nu_{11}\rangle & 0.09 & 0.12 & 0.78 \\ |\nu_2 + \nu_{12}\rangle & 0.45 & 0.34 & 0.22 \\ |2\nu_{10} + \nu_{12}\rangle & 0.46 & 0.54 & 0.00 \end{bmatrix} \tag{56}$$

This spectral region has been measured with high resolution, in the gas phase. Bands having rotational structure consistent with a B_{3u} symmetry vibration have been observed at 2988.6, 3078.5, and 3104.3 cm^{-1}. This agreement is quite good. VPT2+F predicts all three transitions to within about 10 cm^{-1}. This simulation can be taken a bit farther by populating the zero matrix elements of the effective Hamiltonian.

3.2. Darling−Dennison Resonance Constants. Consider the vibrational states ν_{11} and $2\nu_{10} + \nu_{12}$. Their net difference in vibrational quanta is 2. More specifically, when the normal coordinates are considered separately, the number of quanta in q_{12} changes by ±1, the number of quanta in q_{10} changes by ±2, the number of quanta in q_{11} changes by ∓1, and the number of quanta in all other normal coordinates changes by 0. In order for a force constant to couple these states, it must contain an odd number of 11 and 12 indices, an even number (at least two) of q_{10} indices, and an even number (or zero) of other indices. Only one force constant in the anharmonic force field satisfies these criteria, the quartic constant, $\phi_{10,10,11,12}$, of the form ϕ_{rrst}.

In VPT2, these states do not interact, as all coupling between different vibrational states is through cubic terms in the potential. These can connect states differing by 1 and 3 net quanta only. States differing by an even number of net quanta (and zero net quanta) do not interact until VPT4, when quartic couplings between different vibrational states first arise.

In the VPT2+F effective Hamiltonian, these states still do not directly interact; however, they interact indirectly through their mutual coupling to $\nu_2 + \nu_{12}$. The matrix element directly coupling these states has been approximated as zero. Since the force field contains some information about higher-order coupling that is not currently being taken advantage of, it may be desirable to introduce some of this coupling into the model. A simple solution would be to populate this matrix element with $\frac{1}{4\sqrt{2}}\phi_{10,10,11,12}$, where the numerical factor is the usual product of the harmonic oscillator matrix elements, $\frac{1}{2\sqrt{2}}$, the Taylor series coefficient, 1/24, and the degeneracy of the force constant, 12.

A more rigorous approach is to use one of the Darling−Dennison resonance constants, K_{rstu}.[93−96] There are eight types of these. The leading term of each is a quartic force constant (multiplied by the Taylor series coefficient and its degeneracy factor). The remaining terms involve cubic force constants, Coriolis constants, and resonance denominators. These additional terms are derived from perturbation theory (hence the resonance denominators). Their inclusion incorporates more of the correlation effects from VPT4 and is thus more balanced than simply using the quartic force constant (i.e., the cubic and quartic contributions arise at the same order in perturbation theory).

In the ethylene situation, the 1:3 resonance constant, $K_{11;10,10,12}$, is appropriate. Its leading term is $\frac{1}{2}\phi_{10,10,11,12}$, the quartic force constant that couples these vibrational states (without the harmonic oscillator matrix element factor). Before this can be used, it needs to be deperturbed. To do this, search it for resonant terms and zero them out. It is reasonable to use the same diagnostic that is used to deperturb the anharmonicity constants. Resonance constants are kept deperturbed. There is no follow-up matrix-diagonalization step. This particular resonance constant takes the following form (eq 57).

$$\begin{aligned} K_{r;sst} = {} & \frac{1}{2}\phi_{rsst} - \frac{1}{4}\sum_u \phi_{rsu}\phi_{stu}\left(\frac{1}{\omega_r - \omega_s + \omega_u} + \frac{1}{-\omega_r + \omega_s + \omega_u} + \frac{1}{\omega_s + \omega_t + \omega_u} + \frac{1}{-\omega_s - \omega_t + \omega_u}\right) - \frac{1}{8}\sum_u \phi_{rtu}\phi_{ssu}\left(\frac{1}{\omega_r - \omega_t + \omega_u} + \frac{1}{-\omega_r + \omega_t + \omega_u} + \frac{1}{\omega_u + 2\omega_s} + \frac{1}{\omega_u - 2\omega_s}\right) \\ & + 2\sum_\tau (B_e^\tau \zeta_{rs}^\tau \zeta_{st}^\tau)\frac{(\omega_r + \omega_s)(\omega_s - \omega_t)}{\omega_s\sqrt{\omega_r\omega_t}} \end{aligned} \tag{57}$$

https://dx.doi.org/10.1021/acs.jpca.0c09526
J. Phys. Chem. A 2021, 125, 1301−1324

The $K_{r;sst}$ resonance constant connects vibrational states that differ by the annihilation of one quantum in one mode, the creation of one quantum in a different mode, and the creation of two quanta in a third mode. The final matrix element will be the product of this resonance constant and the harmonic oscillator matrix elements.

The expressions for all of the resonance constants and general formulas for all Darling−Dennison matrix elements can be found in the 2014 paper by Rosnik and Polik (Tables 3 and 2 in their article, respectively).[93] Two of the resonance constants in their paper, $K_{kl;mn}$ and $K_{k;lmn}$, have typographical errors. As with the transition moment error addressed in section 2.6.3, these errors are also apparent because these constants do not have the proper permutational symmetry. The value of $K_{kl;mn}$ ought to be invariant to permutation of k and l and permutation of m and n. Likewise, $K_{k;lmn}$ should be invariant to all permutations of l, m, and n. In $K_{kl;mn}$, permutational symmetry can be achieved by changing the fourth resonance denominator associated with $\phi_{kmr}\phi_{lmr}$ from $D[-l,-n,r]$ to $D[-l,n,r]$. In $K_{k;lmn}$, permutational symmetry can be achieved by changing the last Coriolis constant from ζ^{α}_{ml} to ζ^{α}_{lm} (equivalent to changing its sign).

Returning to ethylene, the improved effective Hamiltonian and resonance treatment are given below (eqs 58−60).

$$H_{\text{eff}} = \begin{pmatrix} \nu_{11}^{*} & \frac{1}{2\sqrt{2}}\phi_{2,11,12} & \frac{1}{2\sqrt{2}}K_{11;10,10,12} \\ \frac{1}{2\sqrt{2}}\phi_{2,11,12} & (\nu_2+\nu_{12})^{*} & \frac{1}{4}\phi_{2,10,10} \\ \frac{1}{2\sqrt{2}}K_{11;10,10,12} & \frac{1}{4}\phi_{2,10,10} & (2\nu_{10}+\nu_{12})^{*} \end{pmatrix} \tag{58}$$

$$H_{\text{eff}} = \begin{pmatrix} 3001.8 & 44.4 & -3.5 \\ 44.4 & 3064.6 & -13.3 \\ -3.5 & -13.3 & 3085.4 \end{pmatrix} \tag{59}$$

$$\begin{bmatrix} & \mathbf{3100.0} & \mathbf{3073.1} & \mathbf{2978.7} \\ |\nu_{11}\rangle & 0.10 & 0.11 & 0.79 \\ |\nu_2+\nu_{12}\rangle & 0.44 & 0.35 & 0.21 \\ |2\nu_{10}+\nu_{12}\rangle & 0.46 & 0.54 & 0.00 \end{bmatrix} \tag{60}$$

The result does not appear to be worth the extra effort. The highest-frequency transition now agrees a bit better, the middle transition agrees a bit worse, and the lowest-frequency transition is almost unchanged. Approximating this matrix element as 0 was fine in this situation. The simulation can now be called VPT2+K.[93] It is differentiated from VPT2+F in that its effective Hamiltonians contain not only the standard Fermi-type matrix elements composed of cubic force constants but also Darling−Dennison matrix elements with leading quartic force constants. It provides one of the best and most affordable descriptions of anharmonic coupling possible with a quartic expansion of the potential.

3.3. Antisymmetric CH_2 Stretch of Formaldehyde. The anharmonic coupling in formaldehyde is well-understood, thanks to the efforts of Polik and co-workers.[46,97] It is now accepted that the antisymmetric CH_2 stretch, ν_5, is involved in a resonance triad with two combination states: $\nu_2+\nu_6$ and $\nu_3+\nu_6$. These are [C═O stretch + CH_2 wag] and [CH_2 scissor + CH_2 wag], respectively. As with ethylene, this interaction will require at least a 3 × 3 effective Hamiltonian for a proper description. It will be described with a CCSD(T)/ANO2 force field, containing 22 unique cubic and 45 unique quartic force constants. Begin with the Martin Test (Table 4).

Table 4. Fermi Resonances in Formaldehyde[a]

resonance	Γ	energy separation	cubic force constant	variational − perturbational
$\omega_5 \approx \omega_2+\omega_6$	B_2	37.8	−146.7	34.8
$\omega_5 \approx \omega_3+\omega_6$	B_2	202.9	185.8	1.9

[a]All quantities are given in wavenumbers. Resonances were identified with a 1 cm^{-1} threshold Martin Test, shown in the last column.

With a cutoff value of 1 cm^{-1}, the two resonances identified are precisely the same ones discussed in the literature. Calculate the anharmonicity constants and deperturb for these two resonances. Notice that both resonances necessitate removal of terms from $\chi_{5,6}$. The effect of the $\omega_5 \approx \omega_2+\omega_6$ resonance on the constants is given below.

$$\chi_{2,6} = 64.2 \rightarrow \chi^{*}_{2,6} = -6.8,$$
$$\chi_{2,5} = -72.2 \rightarrow \chi^{*}_{2,5} = -1.1,$$
$$\chi_{5,6} = -80.2 \rightarrow \chi^{*}_{5,6} = -9.1$$

The effect of the $\omega_5 \approx \omega_3+\omega_6$ resonance on the constants is given below.

$$\chi_{3,6} = -19.4 \rightarrow \chi^{*}_{3,6} = 1.9,$$
$$\chi_{3,5} = -12.8 \rightarrow \chi^{*}_{3,5} = -34.0,$$
$$\chi_{5,6} = -80.2 \rightarrow \chi^{*}_{5,6} = -101.5$$

And the net effect of both resonances on the $\chi_{5,6}$ constant is shown below.

$$\chi_{5,6} = -80.2 \rightarrow \chi^{*}_{5,6} = -30.4$$

The structure of this effective Hamiltonian is analogous to the B_2 example from cyclopentadiene. Here, the singly excited vibrational state directly interacts with two doubly excited states via matrix elements containing cubic force constants. This VPT2+F simulation gives very good agreement with experiment (eqs 61−63). The stretch fundamental is observed at 2843 cm^{-1}, and the two combination bands are observed at 3000 and 2719 cm^{-1}. Filling in the 0s of this effective Hamiltonian will be somewhat more involved than in the previous example.[98]

$$H_{\text{eff}} = \begin{pmatrix} \nu_5^{*} & \frac{1}{2\sqrt{2}}\phi_{2,5,6} & \frac{1}{2\sqrt{2}}\phi_{3,5,6} \\ \frac{1}{2\sqrt{2}}\phi_{2,5,6} & (\nu_2+\nu_6)^{*} & \approx 0 \\ \frac{1}{2\sqrt{2}}\phi_{3,5,6} & \approx 0 & (\nu_3+\nu_6)^{*} \end{pmatrix} \tag{61}$$

$$H_{\text{eff}} = \begin{pmatrix} 2828.0 & -51.8 & 65.7 \\ -51.8 & 2987.4 & 0 \\ 65.7 & 0 & 2751.9 \end{pmatrix} \tag{62}$$

https://dx.doi.org/10.1021/acs.jpca.0c09526
J. Phys. Chem. A 2021, 125, 1301−1324

$$\begin{bmatrix} & \mathbf{3004.3} & \mathbf{2851.5} & \mathbf{2711.5} \\ |\nu_5\rangle & 0.10 & 0.63 & 0.27 \\ |\nu_2 + \nu_6\rangle & 0.90 & 0.09 & 0.01 \\ |\nu_3 + \nu_6\rangle & 0.01 & 0.28 & 0.72 \end{bmatrix} \tag{63}$$

3.4. Derivation of a Darling−Dennison Matrix Element. Consider the doubly excited vibrational states $\nu_2 + \nu_6$ and $\nu_3 + \nu_6$. Their net difference in quanta is 0. More specifically, when the normal coordinates are considered separately, the number of quanta in q_2 changes by ± 1, the number of quanta in q_3 changes by ∓ 1, and the number of quanta in q_6 (and all other normal coordinates) changes by 0. Force constants capable of coupling these states will contain an odd number of 2 and 3 indices and an even number (or zero) of all other indices.

In contrast to the 1:3 resonance example in ethylene, there are now multiple quartic force constants that can couple these states. Every constant of the form $\phi_{2,n,3,n}$ can contribute to this matrix element. This matrix element will be a sum of $3N - 6$ resonance constants. It will be simpler to evaluate the harmonic oscillator matrix element "q-factors" separately for each resonance constant that appears. It is important to be aware that, in force constants, the order of the indices does not matter. For resonance constants, the order of the indices (i.e., which side of the semicolon they appear on) does matter. Four possible cases are shown below.

$$n = 2: \quad \text{Resonance constant: } K_{3,2;2,2} \quad q\text{-factor: } \frac{3}{4}$$

$$n = 3: \quad \text{Resonance constant: } K_{2,3;3,3} \quad q\text{-factor: } \frac{3}{4}$$

$$n = 6: \quad \text{Resonance constant: } K_{2,6;3,6} \quad q\text{-factor: } \frac{3}{4}$$

$$n \neq \{2, 3, 6\}: \quad \text{Resonance constant: } K_{2,n;3,n} \quad q\text{-factor: } \frac{1}{4}$$

The final matrix element is defined with all numerical factors absorbed into it.

$$D_{2,6;3,6} = \frac{3}{4}K_{2,3;3,3} + \frac{3}{4}K_{3,2;2,2} + \frac{3}{4}K_{2,6;3,6} + \frac{1}{4}\sum_{n\neq\{2,3,6\}} K_{2,n;3,n} \tag{64}$$

The first two terms in eq 64 are instances of the $K_{rs;ss}$ resonance constant, whereas the third term and the summation use $K_{rt;st}$ constants. The equation differs from eq 20 in ref 98, which was printed incorrectly. This matrix element is similar to the matrix element for resonance between singly excited states; the extra excitation in q_6 simply leads to a higher weight for the $K_{2,6;3,6}$ resonance constant. There is no generally accepted notation for these matrix elements; here they will be denoted by D, for Darling−Dennison. Since formaldehyde is small, the fully expanded matrix element is shown (eq 65).

$$D_{2,6;3,6} = \frac{1}{4}K_{2,1;3,1} + \frac{3}{4}K_{3,2;2,2} + \frac{3}{4}K_{2,3;3,3} + \frac{1}{4}K_{2,4;3,4} + \frac{1}{4}K_{2,5;3,5} + \frac{3}{4}K_{2,6;3,6} \tag{65}$$

$$D_{2,6;3,6} = \frac{1}{4}(32.9) + \frac{3}{4}(-7.4) + \frac{3}{4}(-3.7) + \frac{1}{4}(-3.1) + \frac{1}{4}(36.9) + \frac{3}{4}(-7.9)$$

$$D_{2,6;3,6} = 2.5\text{cm}^{-1}$$

The VPT2+K effective Hamiltonian and resonance treatment are shown below (eqs 66−68). Including the Darling−Dennison matrix element changes almost nothing. It is desirable to now discuss an example where higher-order effects are important (section 3.5).

$$H_{\text{eff}} = \begin{pmatrix} \nu_5^* & \frac{1}{2\sqrt{2}}\phi_{2,5,6} & \frac{1}{2\sqrt{2}}\phi_{3,5,6} \\ \frac{1}{2\sqrt{2}}\phi_{2,5,6} & (\nu_2 + \nu_6)^* & D_{2,6;3,6} \\ \frac{1}{2\sqrt{2}}\phi_{3,5,6} & D_{2,6;3,6} & (\nu_3 + \nu_6)^* \end{pmatrix} \tag{66}$$

$$H_{\text{eff}} = \begin{pmatrix} 2828.0 & -51.8 & 65.7 \\ -51.8 & 2987.4 & 2.5 \\ 65.7 & 2.5 & 2751.9 \end{pmatrix} \tag{67}$$

$$\begin{bmatrix} & \mathbf{3003.9} & \mathbf{2852.3} & \mathbf{2711.1} \\ |\nu_5\rangle & 0.09 & 0.63 & 0.27 \\ |\nu_2 + \nu_6\rangle & 0.90 & 0.09 & 0.01 \\ |\nu_3 + \nu_6\rangle & 0.00 & 0.28 & 0.72 \end{bmatrix} \tag{68}$$

3.5. Doubly and Triply Excited Stretching Levels of Water. This example is borrowed from Matthews, Vazquez, and Stanton.[20] A CCSD(T)/ANO1 quartic force field is used, identical to theirs. Note that because water has fewer than four vibrational degrees of freedom, the incomplete quartic force fields computed by most software packages are identical to a full quartic force field. It contains 6 unique cubic and 9 unique quartic force constants. In accordance with the spectroscopic convention, the symmetric stretch will be referred to as ν_1, and the antisymmetric stretch will be called ν_3.

Begin by computing the Martin diagnostics. Nothing is flagged with a cutoff value of 1 cm^{-1}. If the threshold is loosened to 0.5 cm^{-1}, the symmetric stretch and the bend overtone show up as a resonance. However, an effective Hamiltonian treatment of this interaction will not be necessary. Indeed, if this "resonance" were to be treated, the fundamental would remain 97% pure. The discussion will proceed without any Fermi resonances. Calculate the anharmonicity constants. Contrary to the Fermi resonances encountered earlier, the Darling−Dennison resonances important in this system do not lead to near-zero denominators in the anharmonicity constants. There is nothing that needs to be deperturbed.

The doubly excited stretching levels are well-separated in energy from all triply excited levels. On the basis of their energy differences, it will be a good approximation to separate excited stretching levels into polyads by their net excitation level. Accordingly, the first effective Hamiltonian will contain $2\nu_1$, $\nu_1 + \nu_3$, and $2\nu_3$. Symmetry makes this problem rather easy. Only the matrix element connecting the two A_1 states can be nonzero. This matrix element uses the $K_{rr;ss}$ resonance constant because

https://dx.doi.org/10.1021/acs.jpca.0c09526
J. Phys. Chem. A 2021, 125, 1301−1324

these states are connected by the annihilation of two quanta in one mode and the creation of two quanta in a different mode.

Resonance treatment is shown below (eqs 69−71). To understand the effect of treating the Darling−Dennison resonance, the VPT2+K eigenvalues can be directly compared to the diagonal values (which correspond to the full VPT2 prediction). The Darling−Dennison interaction causes the first overtones to repel each other by 30 cm^{-1}. This pushes them into excellent agreement with the experimental values of 7202 and 7445 cm^{-1}. The uncoupled B_2 combination also matches experiment (7251 cm^{-1}).

$$H_{\text{eff}} = \begin{pmatrix} 2\nu_1 & 0 & \frac{1}{2}K_{1,1;3,3} \\ 0 & (\nu_1 + \nu_3) & 0 \\ \frac{1}{2}K_{1,1;3,3} & 0 & 2\nu_3 \end{pmatrix} \tag{69}$$

$$H_{\text{eff}} = \begin{pmatrix} 7233.6 & 0 & -80.4 \\ 0 & 7250.5 & 0 \\ -80.4 & 0 & 7416.1 \end{pmatrix} \tag{70}$$

$$\begin{bmatrix} & \mathbf{7446.4} & \mathbf{7250.5} & \mathbf{7203.2} \\ |2\nu_1\rangle & 0.12 & 0 & 0.88 \\ |\nu_1 + \nu_3\rangle & 0 & 1.00 & 0 \\ |2\nu_3\rangle & 0.88 & 0 & 0.12 \end{bmatrix} \tag{71}$$

Resonance treatment for the v = 3 polyad is detailed below (eqs 72−74). Again, symmetry helps here. This problem can be block-diagonalized into one 2 × 2 block of each symmetry type (A_1 and B_2). Notice that these matrix elements involve the very same resonance constant from the v = 2 polyad, as the coupled states still differ by creation/annihilation of two quanta in two modes. However, the harmonic oscillator integral factors are larger as a consequence of the greater excitation.

$$H_{\text{eff}} = \begin{pmatrix} 3\nu_1 & 0 & \frac{3}{2\sqrt{3}}K_{1,1;3,3} & 0 \\ 0 & (2\nu_1 + \nu_3) & 0 & \frac{3}{2\sqrt{3}}K_{1,1;3,3} \\ \frac{3}{2\sqrt{3}}K_{1,1;3,3} & 0 & (\nu_1 + 2\nu_3) & 0 \\ 0 & \frac{3}{2\sqrt{3}}K_{1,1;3,3} & 0 & 3\nu_3 \end{pmatrix} \tag{72}$$

$$H_{\text{eff}} = \begin{pmatrix} 10722.2 & 0 & -139.3 & 0 \\ 0 & 10658.6 & 0 & -139.3 \\ -139.3 & 0 & 10743.6 & 0 \\ 0 & -139.3 & 0 & 10977.2 \end{pmatrix} \tag{73}$$

$$\begin{bmatrix} & \mathbf{11029.6} & \mathbf{10872.6} & \mathbf{10606.3} & \mathbf{10593.2} \\ |3\nu_1\rangle & 0 & 0.46 & 0 & 0.54 \\ |2\nu_1 + \nu_3\rangle & 0.12 & 0 & 0.88 & 0 \\ |\nu_1 + 2\nu_3\rangle & 0 & 0.54 & 0 & 0.46 \\ |3\nu_3\rangle & 0.88 & 0 & 0.12 & 0 \end{bmatrix} \tag{74}$$

The B_2 states mix modestly with each other and are corrected by 52 cm^{-1}. However, the uncoupled A_1 states were much closer to each other, so they receive corrections of 129 cm^{-1} and mix thoroughly. The B_2 transitions have been observed at 10 613 and 11 032 cm^{-1}, and A_1 transitions have been identified at 10 600 and 10 869 cm^{-1}. The agreement is less good, but VPT2+K is still capable of predicting these transitions to within 10 cm^{-1}.

By v = 3, it is clear that unacceptable error is introduced by neglecting the Darling−Dennison interaction. And as the excitation level increases, both the density of states and the magnitude of the Darling−Dennison matrix elements increase. With increasing energy and excitation, all simulations based upon VPT2 will eventually break down; however, VPT2+K remains useful for longer.

3.6. A Simpler Procedure for Deperturbation. For systems that involve many resonances, the standard deperturbation procedure entails many manipulations to the anharmonicity constants and becomes cumbersome and error-prone. There is a much more straightforward alternative to deperturbing the anharmonicity constants. All it requires is that VPT2 be understood in both its sum-over-states formulation and in its anharmonicity constant based formulation. First, the structure of the effective Hamiltonian matrices must be deduced from the list of defined Fermi resonances. Then, the fully perturbed diagonal elements are evaluated with the anharmonicity constant based expression, as this is much faster than performing the sum-over-states. Now, the diagonal elements themselves can simply be adjusted by subtracting the SoS VPT2 correction (eq 75) for their interaction with all other states, c, involved in the effective Hamiltonian.

$$\sum_{c \neq a} \frac{|\langle a|\hat{H}_1|c\rangle|^2}{\epsilon_a - \epsilon_c} \tag{75}$$

Now it is not necessary to even use the term "deperturb". It is also appealing that every interaction takes the same form, as opposed to applying tailored corrections for Type I and Type II Fermi resonances to different numbers of anharmonicity constants as is done in the standard procedure. Another advantage of this approach is that it allows for easier modification of the list of resonances and the effective Hamiltonians. One might consider this approach to prioritize the solution of the reduced dimensional coupling problem(s) over all else. As a takeaway message, it is often useful to consider the sensitivity of anharmonic predictions to the choice of resonances and to the extent of effective Hamiltonian treatment. The resonance treatment should be understood as an additional source of uncertainty when critically evaluating VPT predictions.

3.7. Systems of Interacting Resonances. The purpose of this section is to further discuss the relationships between Fermi resonances and to illustrate a few more complicated resonance situations. It is useful to consider the structure of effective Hamiltonian matrices that are implied by certain definitions of resonances. As was seen in the various examples above, when

https://dx.doi.org/10.1021/acs.jpca.0c09526
J. Phys. Chem. A 2021, 125, 1301−1324

several Fermi resonances are active in a system, and these resonances involve some of the same normal coordinates, complicated resonance polyads may result. We might say that the resonances are "connected" to each other through their shared normal coordinates. The ethylene example illustrates a "vertical" connected resonance, necessitating an effective Hamiltonian that couples a one-quantum state to a two-quanta state to a three-quanta state. In contrast, the formaldehyde example shows a "horizontal" connected resonance, implying an effective Hamiltonian treatment of a one-quantum state coupled to two different two-quanta states. These cases can be combined and/or extended to include several different tiers of coupling. For example, consider the following case of a two-level vertical resonance system, having the following active Fermi resonances.

$$\omega_a \approx 2\omega_b \quad \text{and} \quad \omega_b \approx 2\omega_c$$

In complicated situations such as the above, it is most useful to think about the list of resonances as a list of replacement rules. Iterate through the states in the effective Hamiltonian, replacing indices with resonant indices to generate new states, until all possible resonant states are present. An effective Hamiltonian that simultaneously couples all of these states will provide a theoretically "complete" treatment of the resonance system. Equations 76 and 77 show how predictions for various states might be made, in the presence of this resonance system. Treatment of vertical resonances demands the coupling of states with successively higher levels of excitation. Discussion of the treatment of complicated resonance polyads is scarce in the literature; however, examples can be found in ref 99 and in the Supporting Information of ref 87.

$$H_{\text{eff}} = \begin{pmatrix} \nu_b^* & \frac{1}{4}\phi_{bcc} \\ \frac{1}{4}\phi_{bcc} & 2\nu_c^* \end{pmatrix} \tag{76}$$

$$H_{\text{eff}} = \begin{pmatrix} \nu_a^* & \frac{1}{4}\phi_{abb} & \frac{1}{2\sqrt{2}}K_{a;bcc} & 0 \\ \frac{1}{4}\phi_{abb} & 2\nu_b^* & \frac{1}{2\sqrt{2}}\phi_{bcc} & 0 \\ \frac{1}{2\sqrt{2}}K_{a;bcc} & \frac{1}{2\sqrt{2}}\phi_{bcc} & (\nu_b + 2\nu_c)^* & \frac{\sqrt{3}}{2\sqrt{2}}\phi_{bcc} \\ 0 & 0 & \frac{\sqrt{3}}{2\sqrt{2}}\phi_{bcc} & 4\nu_c^* \end{pmatrix} \tag{77}$$

In some automated implementations of variationally corrected VPT2, such as GVPT2, the couplings to excited states of three quanta and greater are not treated in a variational framework; rather, the two-quantum states are left partially deperturbed.[32] While it is more appealing to treat the couplings, it is doubtful that very high levels of excitation (e.g., couplings with six-quanta states and higher) will lead to higher-accuracy predictions, as the description of increasingly higher excited states, based merely upon a quartic expansion of the potential, becomes increasingly poor. Sometimes it may be wise to truncate the list of resonances in order to prevent the effective Hamiltonian from becoming too large. Complicated resonance treatments should not always be avoided; however, they should be taken with a grain of salt. If a system is subjected to various reasonable resonance treatments, and a particular transition frequency shows high sensitivity, then that prediction should be taken to be less certain.

Finally, it is an interesting fact that certain systems of resonances are impossible to treat in a complete and satisfying manner. Consider below the case of the cyclic resonance.

$$\omega_a \approx \omega_b + \omega_c \qquad \omega_b \approx \omega_a + \omega_c \qquad \omega_c \approx \omega_a + \omega_b$$

Attempting to build an effective Hamiltonian to treat this system of resonances leads to an infinite number of substitutions and inclusion of states that are infinitely excited. There are no real systems where a cyclic resonance would be a reasonable model of the anharmonic coupling. However, the Martin Test has a tendency to identify these cyclic resonances in systems with low-frequency modes (e.g., alkyl radicals). By combining the Martin Test with an energy window test (often with a 200 cm^{-1} threshold), cyclic resonances are effectively eliminated.[32,98,100]

3.8. Large Effective Hamiltonian Simulations. *3.8.1. Description.* This section discusses a philosophy and standard procedure for predicting the CH stretching (~2700−3150 cm^{-1}) spectra of hydrocarbons, which employs VPT2+K with large effective Hamiltonians. This is a particularly robust and accurate approach for small alkenes, where it allows for excellent quality intensity predictions, even when using harmonic oscillator transition moments. An application to isoprene is made in section 3.8.2. Variations of this approach are also applied in several manuscripts.[5,13,88,101−103]

The use of large VPT2+K effective Hamiltonians was inspired by work in the Sibert group[104] on modeling CH stretch Fermi coupling with local mode models.[5] The most significant anharmonic interactions involving CH stretch fundamentals are assumed to be their couplings with doubly excited HCH bending states (sometimes called scissors). The most basic local-mode model of Sibert and co-workers, referred to as the "simple model", will be the subject of all further discussion of local mode models.[104] In this model, a methyl group contributes three scissor coordinates, a methylene group (either bridging or terminal radical) contributes one scissor coordinate, and other functional groups do not contribute. From the pool of X scissoring coordinates generated, all possible doubly excited scissoring states are generated, totaling $(1/2)X(X + 1)$ states, where X states are overtones, and the remainder are combinations. These are mutually coupled together and with the CH stretch fundamentals in an effective Hamiltonian.

When this large effective Hamiltonian treatment of anharmonic coupling is adapted for VPT2+K in normal coordinates, the resulting model is more flexible; however, it produces more complicated effective Hamiltonians. The increased flexibility is a consequence of its *ab initio* nature, contrasting with the local-mode model. This allows for couplings to other kinds of coordinates to be treated straightforwardly without requiring parametrization. For instance, coupling to [HCH scissor + C═C stretch] states proves to be quite important in alkenes (section 3.8.2), and it can be accounted for by simply expanding the pool of coordinates to include the C═C stretch.[101,103] The option to include Darling−Dennison coupling also increases the model's flexibility; however, the significance of these couplings in the CH stretching region is generally minor.[5] In VPT2+K, more complicated effective Hamiltonians often arise due to the explicit consideration of Fermi resonances other than those between CH stretches and HCH bends. As described in section 3.7, connected Fermi resonances necessitate the consideration of additional coordinates and the explicit coupling of multiply excited states. For

https://dx.doi.org/10.1021/acs.jpca.0c09526
J. Phys. Chem. A 2021, 125, 1301−1324

comparison, the local mode model will always have the advantage of not requiring the evaluation of expensive anharmonic force fields. Moreover, the interpretation of couplings is simplified in comparison to the localized nature of the coordinate system. The local mode model is valuable not only as an effective standalone simulation of Fermi coupling but optionally as a companion to *ab initio* VPT2+K.

The recent work of Lee and co-workers on infrared spectroscopy of polycyclic aromatic hydrocarbons (PAH) is deserving of mention.[105−108] To describe the CH stretching spectra of these molecules, a similar variationally corrected VPT2 model was used, also leading to large polyads. Some important differences include that their work was based on DFT force fields (necessitated by the large size of the PAH molecules), resonance identification was based on separate force constant and energy different thresholds, and the effects of connected resonances were not considered. The quality of their CH stretching predictions was generally quite good and allowed for confident assignments of the majority of the transitions.

3.8.2. Application to trans-Isoprene. A final example is presented in this section. A comparison is made between VPT2 simulations of the CH stretching region of isoprene with varying extents of effective Hamiltonian resonance treatment. In order to make this comparison as fair as possible, VPT2-quality transition moments are used in all simulations (except the last) for one- and two-quanta transitions. This entails that the intensities of all "resonant" transitions are obtained from diagonalized-projected DVPT2 transition moments,[46] and "nonresonant" transition intensities are obtained directly from VPT2 transition moments. A CCSD(T)/ANO[1,0] quartic force field is used with the substituted hybrid scheme. Dipole derivatives are determined at the CCSD(T)/ANO0 level of theory. Small amounts of *gauche*-isoprene are present in the experimental spectrum, but no attempt is made here to account for its absorptions. Transitions of *gauche*-isoprene are identified in three regions of the spectrum and are indicated with arrows. From left to right, the arrows designate: (i) The small peak with low signal-to-noise. (ii) Either the weaker, sharper peak or the red shoulder on the stronger peak. (iii) Both the weak peak and the blue shoulder on the strong peak. A more detailed treatment of the two conformers, including assignments, magnified spectral regions, and VPT2+K predictions for *gauche*-isoprene has been published elsewhere.[103]

To start, it is desirable to show a simulation that is representative of the minimalist treatment of anharmonic resonances that prevails in the literature. In order to do this, a more primitive resonance diagnostic is used for Fermi resonances. The zeroth-order states are considered to be in resonance if two conditions are met: (i) They are separated in energy by less than 50 wavenumbers. (ii) The cubic force constant that couples them has a magnitude of greater than 50 wavenumbers. This diagnostic identifies three Fermi resonances; five vibrational states receive effective Hamiltonian treatment. Below, the corresponding VPT2+F simulation is compared to an experimental spectrum (Figure 3, trace a).

This simulation fails to capture the spectral complexity—especially in the regions centered around 2900 and 3050 cm^{-1}. These regions are predicted to have single, strong transitions; however, the experiment contains many weaker transitions instead. The two strong, high-frequency features correspond to the antisymmetric CH_2 stretches, and these are predicted accurately. Also, the strong experimental transition at 2958 cm^{-1} corresponds to the strong theoretical prediction at 2950 cm^{-1}. This is the sole CH stretching fundamental of a″ symmetry and

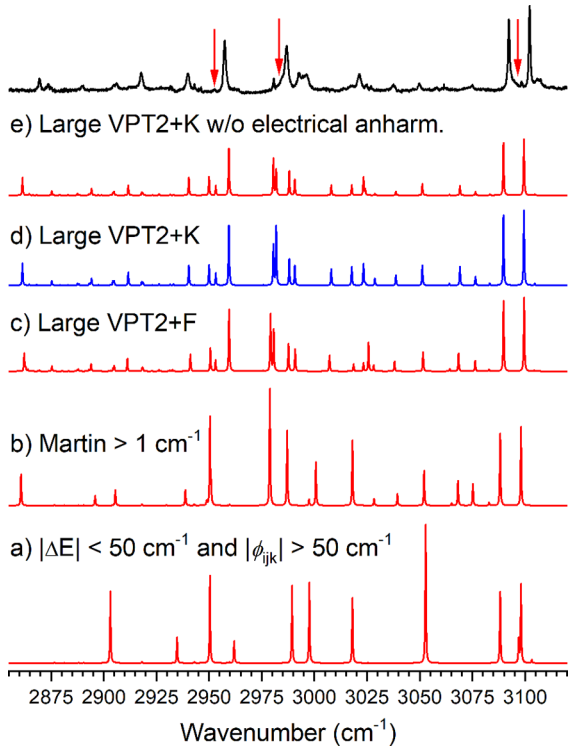

Figure 3. Infrared spectrum of isoprene compared to various VPT2 simulations. The most rigorous simulation is shown in blue. (a) VPT2+F based on individual energy difference and force constant magnitude tests. (b) VPT2+F based on Martin test. (c) VPT2+F based on the "large effective Hamiltonian" model. (d) VPT2+K based on the "large effective Hamiltonian" model. (e) VPT2+K based on the "large effective Hamiltonian" model and assuming electrical harmonicity.

does not participate in extensive resonances. A detailed discussion of assignments has been published.[103] The remaining discussion in this section will evaluate how well VPT2 models the spectral patterns, with only little regard for what the underlying transitions are assigned to.

It is reasonable to think that a better description might be achieved by using the Martin Test to identify the Fermi resonances (*vide supra*). With the standard 1 cm^{-1} threshold, a total of 17 resonances are identified, which are relevant to the CH stretching region. An effective Hamiltonian treatment of these resonances involves the coupling of 20 vibrational states. A comparison is made between a VPT2+F simulation based on this list of resonances (Figure 3, trace b) and the previous VPT2+F simulation. The simulation changes dramatically for the better. The 3050 cm^{-1} region is now well-populated by weak transitions; these generally agree well with experiment. Similar changes are observed in the 2900 cm^{-1} region; however, the agreement is less good. Lastly, the patterns also change on both sides of the spectral valley at 2970 cm^{-1}.

Next, the large effective Hamiltonian model is applied, combined with the 1 cm^{-1} Martin Test to identify connected resonances (Figure 3, trace c). In this model, the effective Hamiltonian mutually couples 8 one-quantum states, 45 two-quanta states, 60 three-quanta states, and 20 four-quanta states, for a total of 133 vibrational states. The features from 2970 to 3030 cm^{-1} are much better described with the larger Hamiltonian. Moreover, inspection of the effective Hamiltonian eigenvectors suggests that these features are highly anharmonic, involving complicated mixtures of four of the zeroth-order CH

https://dx.doi.org/10.1021/acs.jpca.0c09526
J. Phys. Chem. A 2021, 125, 1301−1324

stretches. The mixing of the CH stretches is achievable entirely through indirect coupling, as the 1:1 Darling−Dennison matrix elements have not yet been included.

The lone fundamental of a″ symmetry now agrees better with experiment. The low-frequency region is also improved; roughly the correct number of intense transitions are now predicted in this region. This comparison is somewhat qualitative, of course, as the low-frequency experimental transitions are weak and difficult to identify. Also note the large effective Hamiltonian model predicts the doublet feature centered around 2870 cm^{-1}, whereas the Martin Test simulation predicts only a single, strong transition.

Darling−Dennison couplings are then introduced into the large effective Hamiltonian, upgrading VPT2+F to VPT2+K (Figure 3, trace d). Only the frequency predictions of the 3020 cm^{-1} feature prove sensitive to the inclusion of Darling−Dennison coupling. This feature arises from several partially overlapping transitions. Because of the variable broadening in the experimental spectrum, it is difficult to judge which of the two simulations is more accurate here. The relative intensities of the two predicted transitions around 2980 cm^{-1} also switch. This is a result of the coupling between two close-lying states being slightly adjusted by small Darling−Dennison terms. Intensity predictions are often sensitive in regions where the density of vibrational states is high.

Clearly, the VPT2 simulations for isoprene, based on large effective Hamiltonians, are far superior to those that opt to treat only the most severe Fermi resonances. Specifically, large effective Hamiltonian VPT2 simulations provide much more accurate intensity predictions than standard VPT2, even when the intensities are determined from VPT2 transition moments. It is interesting to compare the current "best" large effective Hamiltonian VPT2+K simulation to a simulation in which the intensity is derived from only linear harmonic oscillator transition moments (Figure 3, trace e). A qualitative comparison of the two simulations reveals that the VPT2 transition moments are indeed better, except perhaps for the two transitions predicted around 3060 cm^{-1}, where harmonic intensity provides a closer match to experiment. However, the intensity predictions are not sufficiently better with VPT2 transition moments such that it changes the interpretation of the spectrum (i.e., the assignments of the experimental bands). The far simpler harmonic intensity is arguably "good enough" for the purposes of assigning the spectrum. Considering that VPT2 transition moments are highly resonance-prone, this can make them difficult to trust. This is especially true for larger molecular systems with high densities of states. Although it is possible to eliminate resonance denominators from VPT2 transition moments with carefully chosen numerical thresholds, the harmonic intensity is appealing for its simplicity. The use of harmonic oscillator transition moments combined with large effective Hamiltonians is thus generally recommended for the prediction of CH stretches. VPT2 transition moments are recommended if very high accuracy is desired.

Similar to VPT2 transition moments, the inclusion of Darling−Dennison couplings in the CH stretching region may also be considered optional. The expressions for the Darling−Dennison resonance constants are algebraically complicated and require deperturbation; however, they are all simpler in both respects than the one- and three-quanta VPT2 transition moments. The accuracy of VPT2+F is not greatly inferior to VPT2+K in the CH stretching fundamental region.

4. CONCLUSIONS

Theoretical background, equations, and recommendations have been given for the use of the second-order vibrational perturbation theory with resonances (VPT2+K) anharmonic model.[93] Many examples were given of its successful application to molecules with varying severity of anharmonic resonance. Particular attention was paid to setting up effective Hamiltonians for systems with multiple, interacting Fermi resonances. Analytic expressions for VPT2 transition moments between the ground state and three-quanta states were reported together, in their correct form, for the first time. The one-quantum and two-quanta formulas were reproduced alongside them.

In modeling the CH stretch regions of hydrocarbons with large effective Hamiltonian simulations, the significance of Darling−Dennison couplings could be explored. Their contribution was found to be minimal in the CH stretching region. Although a detailed benchmarking study has not been performed, it is expected that theoretical models that neglect Darling−Dennison coupling will still be very successful here. The intensities in these hydrocarbon systems were derived from both linear harmonic oscillator transition moments and VPT2 transition moments. The agreement with experiment is sufficiently good to facilitate spectral assignment with the simpler harmonic oscillator transition moments. The far more complicated deperturbed VPT2 transition moments do not appear to be necessary for simulations of CH stretches.[46] It may even be the case that large effective Hamiltonian simulations using harmonic oscillator transition moments provide superior predictions to small effective Hamiltonian simulations based on more rigorous transition moments, which appears to be the more prevalent choice in the literature. Similar ideas about the adequacy of electrical harmonicity have been expressed by Lee, Tielens, and co-workers.[108]

In small alkenes, strong Fermi couplings occur between the highest-frequency CH stretches and combinations involving both C=C stretching and CH_2 bending.[101] In isoprene, this is found to be the dominant type of anharmonic coupling in the region above 3050 cm^{-1}. In propene, a Fermi resonance of this type also causes the antisymmetric CH_2 stretch fundamental to split into two strong features.[101] This likely generalizes to larger alkenes. In both systems, VPT2+K also predicts that there is a moderate tendency for the CH stretches to mix among themselves. Most of this mixing is due to indirect coupling rather than to direct Darling−Dennison coupling. Such a thing is permitted by large effective Hamiltonians but is missed entirely in simulations that attempt to distill the anharmonic coupling problem down to a series of simple two- or three-state interactions.

Some of the topics discussed in this article would benefit from dedicated theoretical study and benchmarking efforts. It would be particularly valuable to establish the errors associated with different types of hybrid force field approximations and also to find more effective combinations of high and low levels of theory. The viability of large effective Hamiltonian simulations for other kinds of molecules would also be worthwhile to investigate; preliminary work suggests that the approach is somewhat less successful for alkanes. Variationally corrected VPT4 is currently being considered. A similar model to VPT2+F is readily obtained from VPT4; however, a partial incorporation of VPT6 correlation (a method analogous to VPT2+K) has not yet been realized. Expressions for transition moments and some rovibrational constants are not currently known for VPT4. For

https://dx.doi.org/10.1021/acs.jpca.0c09526
J. Phys. Chem. A 2021, 125, 1301−1324

use with VPT4, efficient and accurate implementations of sextic force field computations are also lacking.

■ ASSOCIATED CONTENT

Supporting Information

The Supporting Information is available free of charge at https://pubs.acs.org/doi/10.1021/acs.jpca.0c09526.

Corrected analytic expressions for VPT2 transition moments (PDF)

■ AUTHOR INFORMATION

Corresponding Author

Gary E. Douberly − *Department of Chemistry, University of Georgia, Athens, Georgia 30602, United States;* orcid.org/0000-0001-6530-7466; Phone: 01-706-542-3857; Email: douberly@uga.edu

Authors

Peter R. Franke − *Department of Chemistry, University of Florida, Gainesville, Florida 32611, United States; Department of Chemistry, University of Georgia, Athens, Georgia 30602, United States*

John F. Stanton − *Department of Chemistry, University of Florida, Gainesville, Florida 32611, United States*

Complete contact information is available at: https://pubs.acs.org/10.1021/acs.jpca.0c09526

Notes

The authors declare no competing financial interest.

■ ACKNOWLEDGMENTS

We acknowledge support from the National Science Foundation (GED; CHE-1664637, JFS; CHE-1664325) and the US Department of Energy (DOE), Office of Science, Office of Basic Energy Sciences (BES) under Contract Nos. DE-SC0018412 (GED) and DE-FG02-07ER15884 (JFS).

■ REFERENCES

(1) Wilson, E. B., Jr.; Decius, J. C.; Cross, P. C. *Molecular Vibrations: The Theory of Infrared and Raman Vibrational Spectra*; McGraw-Hill, 1955; p 388.

(2) Califano, S. *Vibrational States*; John Wiley & Sons, Ltd., 1976; p 335.

(3) Mills, I. M. *Vibration-Rotation Structure in Asymmetric and Symmetric Top Molecules*; Academic Press, 1972; p 115−140.

(4) Bowman, J. M. The Self-Consistent-Field Approach to Polyatomic Vibrations. *Acc. Chem. Res.* **1986**, *19*, 202−208.

(5) Franke, P. R.; Tabor, D. P.; Moradi, C. P.; Douberly, G. E.; Agarwal, J.; Schaefer, H. F.; Sibert, E. L. Infrared Laser Spectroscopy of the *n*-Propyl and *i*-Propyl Radicals: Stretch-Bend Fermi Coupling in the Alkyl CH Stretch Region. *J. Chem. Phys.* **2016**, *145*, 224304.

(6) Biczysko, M.; Bloino, J.; Puzzarini, C. Computational Challenges in Astrochemistry. *Wiley Interdiscip. Rev.: Comput. Mol. Sci.* **2018**, *8*, e1349.

(7) Raston, P. L.; Agarwal, J.; Turney, J. M.; Schaefer, H. F.; Douberly, G. E. The Ethyl Radical in Superfluid Helium Nanodroplets: Rovibrational Spectroscopy and Ab Initio Computations. *J. Chem. Phys.* **2013**, *138*, 194303.

(8) Tew, D. P.; Handy, N. C.; Carter, S. Glyoxal Studied with 'MULTIMODE', Explicit Large Amplitude Motion and Anharmonicity. *Phys. Chem. Chem. Phys.* **2001**, *3*, 1958−1964.

(9) McDonald, D. C.; Wagner, J. P.; McCoy, A. B.; Duncan, M. A. Near-Infrared Spectroscopy and Anharmonic Theory of Protonated Water Clusters: Higher Elevations in the Hydrogen Bonding Landscape. *J. Phys. Chem. Lett.* **2018**, *9*, 5664−5671.

(10) Guasco, T. L.; Johnson, M. A.; McCoy, A. B. Unraveling Anharmonic Effects in the Vibrational Predissociation Spectra of $H_5O_2^+$ and Its Deuterated Analogues. *J. Phys. Chem. A* **2011**, *115*, 5847−5858.

(11) Colbert, D. T.; Miller, W. H. A Novel Discrete Variable Representation for Quantum-Mechanical Reactive Scattering via the S-Matrix Kohn Method. *J. Chem. Phys.* **1992**, *96*, 1982−1991.

(12) Changala, P. B.; Baraban, J. H. Ab Initio Effective Rotational and Rovibrational Hamiltonians for Non-Rigid Systems via Curvilinear Second Order Vibrational Møller-Plesset Perturbation Theory. *J. Chem. Phys.* **2016**, *145*, 174106.

(13) Brown, A. R.; Franke, P. R.; Douberly, G. E. Helium Nanodroplet Isolation of the Cyclobutyl, 1-Methylallyl, and Allylcarbinyl Radicals: Infrared Spectroscopy and Ab Initio Computations. *J. Phys. Chem. A* **2017**, *121*, 7576−7587.

(14) Li, C. Y.; Agarwal, J.; Wu, C. H.; Allen, W. D.; Schaefer, H. F. Intricate Internal Rotation Surface and Fundamental Infrared Transitions of the *n*-Propyl Radical. *J. Phys. Chem. B* **2015**, *119*, 728−735.

(15) Nielsen, H. H. The Vibration-Rotation Energies of Molecules. *Rev. Mod. Phys.* **1951**, *23*, 90−136.

(16) Watson, J. K. G. Simplification of the Molecular Vibration-Rotation Hamiltonian. *Mol. Phys.* **1968**, *15*, 479−490.

(17) Meyer, H. The Molecular Hamiltonian. *Annu. Rev. Phys. Chem.* **2002**, *53*, 141−172.

(18) Wilson, E. B.; Howard, J. B. The Vibration-Rotation Energy Levels of Polyatomic Molecules I. Mathematical Theory of Semirigid Asymmetrical Top Molecules. *J. Chem. Phys.* **1936**, *4*, 260−268.

(19) Colbert, D. T.; Sibert, E. L. Variable Curvature Coordinates for Molecular Vibrations. *J. Chem. Phys.* **1989**, *91*, 350−363.

(20) Matthews, D. A.; Vazquez, J.; Stanton, J. F. Calculated Stretching Overtone Levels and Darling-Dennison Resonances in Water: A Triumph of Simple Theoretical Approaches. *Mol. Phys.* **2007**, *105*, 2659−2666.

(21) Carbonniere, P.; Barone, V. Coriolis Couplings in Variational Computations of Vibrational Spectra Beyond the Harmonic Approximation: Implementation and Validation. *Chem. Phys. Lett.* **2004**, *392*, 365−371.

(22) Gong, J. Z.; Matthews, D. A.; Changala, P. B.; Stanton, J. F. Fourth-Order Vibrational Perturbation Theory with the Watson Hamiltonian: Report of Working Equations and Preliminary Results. *J. Chem. Phys.* **2018**, *149*, 114102.

(23) Dunham, J. L. The Energy Levels of a Rotating Vibrator. *Phys. Rev.* **1932**, *41*, 721−731.

(24) Schuurman, M. S.; Allen, W. D.; Schleyer, P. V.; Schaefer, H. F. The Highly Anharmonic BH_5 Potential Energy Surface Characterized in the Ab Initio Limit. *J. Chem. Phys.* **2005**, *122*, 104302.

(25) Piccardo, M.; Bloino, J.; Barone, V. Generalized Vibrational Perturbation Theory for Rotovibrational Energies of Linear, Symmetric and Asymmetric tops: Theory, Approximations, and Automated Approaches to Deal with Medium-to-Large Molecular Systems. *Int. J. Quantum Chem.* **2015**, *115*, 948−982.

(26) Martin, J. M. L.; Lee, T. J.; Taylor, P. R.; Francois, J. P. The Anharmonic-Force Field of Ethylene, C_2H_4, by Means of Accurate Ab Initio Calculations. *J. Chem. Phys.* **1995**, *103*, 2589−2602.

(27) Stanton, J. F.; Gauss, J.; Cheng, L.; Harding, M. E.; Matthews, D. A.; Szalay, P. G. *CFOUR, Coupled-cluster techniques for computational chemistry, a quantum-chemical program package*, with the integral packages MOLECULE (J. Almlöf and P. R. Taylor), PROPS (P. R. Taylor), ABACUS (T. Helgaker, H. J. Aa. Jensen, P. Jørgensen, and J. Olsen), and ECP routines by A. V. Mitin and C. van Wüllen, for the current version, see http://www.cfour.de.

(28) Matthews, D. A.; Stanton, J. F. Quantitative Analysis of Fermi Resonances by Harmonic Derivatives of Perturbation Theory Corrections. *Mol. Phys.* **2009**, *107*, 213−222.

(29) Barone, V. Anharmonic Vibrational Properties by a Fully Automated Second-Order Perturbative Approach. *J. Chem. Phys.* **2005**, *122*, 014108.

(30) Burcl, R.; Carter, S.; Handy, N. C. On the Representation of Potential Energy Surfaces of Polyatomic Molecules in Normal Coordinates: II. Parameterisation of the Force Field. *Chem. Phys. Lett.* **2003**, *373*, 357−365.
(31) Gaw, J. F.; Willetts, A.; Green, W. H.; Handy, N. C. SPECTRO version 3.0. In *Advances in Molecular Vibrations and Dynamics*; Bowman, J. M., Ed.; JAI Press: Greenwich, CT, 1990.
(32) Frisch, J.; Trucks, G. W.; Schlegel, H. B.; Scuseria, G. E.; Robb, M. A.; Cheeseman, J. R.; Scalmani, G.; Barone, V.; Mennucci, B.; Petersson, G. A.; et al. *Gaussian 09*, Revision E.01; Gaussian, Inc.: Wallingford, CT, USA, 2009.
(33) Matthews, D. A.; Cheng, L.; Harding, M. E.; Lipparini, F.; Stopkowicz, S.; Jagau, T. C.; Szalay, P. G.; Gauss, J.; Stanton, J. F. Coupled-Cluster Techniques for Computational Chemistry: The CFOUR Program Package. *J. Chem. Phys.* **2020**, *152*, 214108.
(34) Puzzarini, C.; Bloino, J.; Tasinato, N.; Barone, V. Accuracy and Interpretability: The Devil and the Holy Grail. New Routes Across Old Boundaries in Computational Spectroscopy. *Chem. Rev.* **2019**, *119*, 8131−8191.
(35) Biczysko, M.; Krupa, J.; Wierzejewska, M. Theoretical Studies of Atmospheric Molecular Complexes Interacting with NIR to UV Light. *Faraday Discuss.* **2018**, *212*, 421−441.
(36) Bloino, J.; Baiardi, A.; Biczysko, M. Aiming at an Accurate Prediction of Vibrational and Electronic Spectra for Medium-to-Large Molecules: An Overview. *Int. J. Quantum Chem.* **2016**, *116*, 1543−1574.
(37) Kuhler, K. M.; Truhlar, D. G.; Isaacson, A. D. General Method for Removing Resonance Singularities in Quantum Mechanical Perturbation Theory. *J. Chem. Phys.* **1996**, *104*, 4664−4671.
(38) Bloino, J.; Biczysko, M.; Barone, V. General Perturbative Approach for Spectroscopy, Thermodynamics, and Kinetics: Methodological Background and Benchmark Studies. *J. Chem. Theory Comput.* **2012**, *8*, 1015−1036.
(39) McCoy, A. B.; Guasco, T. L.; Leavitt, C. M.; Olesen, S. G.; Johnson, M. A. Vibrational Manifestations of Strong Non-Condon Effects in the $H_3O^+ \bullet X_3$ (X = Ar, N_2, CH_4, H_2O) Complexes: A Possible Explanation for the Intensity in the "Association Band" in the Vibrational Spectrum of Water. *Phys. Chem. Chem. Phys.* **2012**, *14*, 7205−7214.
(40) Kjaergaard, H. G.; Garden, A. L.; Chaban, G. M.; Gerber, R. B.; Matthews, D. A.; Stanton, J. F. Calculation of Vibrational Transition Frequencies and Intensities in Water Dimer: Comparison of Different Vibrational Approaches. *J. Phys. Chem. A* **2008**, *112*, 4324−4335.
(41) Vazquez, J.; Stanton, J. F. Simple(r) Algebraic Equation for Transition Moments of Fundamental Transitions in Vibrational Second-Order Perturbation Theory. *Mol. Phys.* **2006**, *104*, 377−388.
(42) Bloino, J.; Biczysko, M.; Barone, V. Anharmonic Effects on Vibrational Spectra Intensities: Infrared, Raman, Vibrational Circular Dichroism, and Raman Optical Activity. *J. Phys. Chem. A* **2015**, *119*, 11862−11874.
(43) Willetts, A.; Handy, N. C.; Green, W. H.; Jayatilaka, D. Anharmonic Corrections to Vibrational Transition Intensities. *J. Phys. Chem.* **1990**, *94*, 5608−5616.
(44) Green, W. H.; Willetts, A.; Jayatilaka, D.; Handy, N. C. Ab Initio Prediction of Fundamental, Overtone and Combination Band Infrared Intensities. *Chem. Phys. Lett.* **1990**, *169*, 127−137.
(45) Bloino, J.; Barone, V. A Second-Order Perturbation Theory Route to Vibrational Averages and Transition Properties of Molecules: General Formulation and Application to Infrared and Vibrational Circular Dichroism Spectroscopies. *J. Chem. Phys.* **2012**, *136*, 124108.
(46) Vazquez, J.; Stanton, J. F. Treatment of Fermi Resonance Effects on Transition Moments in Vibrational Perturbation Theory. *Mol. Phys.* **2007**, *105*, 101−109.
(47) Bloino, J. A VPT2 Route to Near-Infrared Spectroscopy: The Role of Mechanical and Electrical Anharmonicity. *J. Phys. Chem. A* **2015**, *119*, 5269−5287.
(48) *Mathematica*, Version 11; Wolfram Research, Inc.: Champaign, IL, 2016.
(49) Neese, F. The ORCA Program System. *Wiley Interdiscip. Rev.: Comput. Mol. Sci.* **2012**, *2*, 73−78.
(50) Neese, F. Software Update: The ORCA Program System, Version 4.0. *Wiley Interdiscip. Rev.: Comput. Mol. Sci.* **2018**, *8*, e1327.
(51) Roos, B. O.; Taylor, P. R.; Siegbahn, P. E. M. A Complete Active Space SCF Method (CASSCF) Using a Density-Matrix Formulated Super-CI Approach. *Chem. Phys.* **1980**, *48*, 157−173.
(52) Siegbahn, P. E. M.; Almlof, J.; Heiberg, A.; Roos, B. O. The Complete Active Space SCF (CASSCF) Method in a Newton-Raphson Formulation with Application to The HNO Molecule. *J. Chem. Phys.* **1981**, *74*, 2384−2396.
(53) Lee, T. J.; Taylor, P. R. A Diagnostic for Determining the Quality of Single-Reference Electron Correlation Methods. *Int. J. Quantum Chem.* **1989**, *36*, 199−207.
(54) Cheng, L.; Gauss, J.; Ruscic, B.; Armentrout, P. B.; Stanton, J. F. Bond Dissociation Energies for Diatomic Molecules Containing 3d Transition Metals: Benchmark Scalar-Relativistic Coupled-Cluster Calculations for 20 Molecules. *J. Chem. Theory Comput.* **2017**, *13*, 1044−1056.
(55) Bally, T.; Borden, W. Calculations on Open-Shell Molecules: A Beginner's Guide. In *Rev. Comput. Chem.*; John Wiley & Sons, Inc., 2007; Vol. *13*, pp 1−97.
(56) Krylov, A. I. The Quantum Chemistry of Open-Shell Species. In *Rev. Comput. Chem.*, First ed.; Parrill, A. L., Lipkowitz, K. B., Eds.; John Wiley & Sons, Inc., 2017; Vol. *30*.
(57) Szalay, P. G.; Gauss, J. Spin-Restricted Open-Shell Coupled-Cluster Theory for Excited States. *J. Chem. Phys.* **2000**, *112*, 4027−4036.
(58) Stanton, J. F. On the Extent of Spin Contamination in Open-Shell Coupled-Cluster Wave Functions. *J. Chem. Phys.* **1994**, *101*, 371−374.
(59) Crawford, T. D.; Stanton, J. F.; Allen, W. D.; Schaefer, H. F. Hartree-Fock Orbital Instability Envelopes in Highly Correlated Single-Reference Wave Functions. *J. Chem. Phys.* **1997**, *107*, 10626−10632.
(60) Szalay, P. G.; Vazquez, J.; Simmons, C.; Stanton, J. F. Triplet Instability in Doublet Systems. *J. Chem. Phys.* **2004**, *121*, 7624−7631.
(61) Stanton, J. F.; Gauss, J. A Discussion of Some Problems Associated with the Quantum Mechanical Treatment of Open-Shell Molecules. In *Adv. Chem. Phys.*; Prigogine, I., Rice, S. A., Eds.; John Wiley & Sons, Inc., 2003; Vol. *125*.
(62) Margraf, J. T.; Perera, A.; Lutz, J. J.; Bartlett, R. J. Single-Reference Coupled Cluster Theory for Multi-Reference Problems. *J. Chem. Phys.* **2017**, *147*, 184101.
(63) Dykstra, C. E. Examination of Brueckner Condition for Selection of Molecular-Orbitals in Correlated Wavefunctions. *Chem. Phys. Lett.* **1977**, *45*, 466−469.
(64) Krylov, A. I. Equation-of-Motion Coupled-Cluster Methods for Open-Shell and Electronically Excited Species: The Hitchhiker's Guide to Fock Space. *Annu. Rev. Phys. Chem.* **2008**, *59*, 433−462.
(65) Howard, J. C.; Gray, J. L.; Hardwick, A. J.; Nguyen, L. T.; Tschumper, G. S. Getting down to the Fundamentals of Hydrogen Bonding: Anharmonic Vibrational Frequencies of $(HF)_2$ and $(H_2O)_2$ from Ab Initio Electronic Structure Computations. *J. Chem. Theory Comput.* **2014**, *10*, 5426−5435.
(66) Tajti, A.; Szalay, P. G.; Csaszar, A. G.; Kallay, M.; Gauss, J.; Valeev, E. F.; Flowers, B. A.; Vazquez, J.; Stanton, J. F. HEAT: High Accuracy Extrapolated Ab Initio Thermochemistry. *J. Chem. Phys.* **2004**, *121*, 11599−11613.
(67) Karton, A.; Rabinovich, E.; Martin, J. M. L.; Ruscic, B. W4 Theory for Computational Thermochemistry: In Pursuit of Confident sub-kJ/mol Predictions. *J. Chem. Phys.* **2006**, *125*, 144108.
(68) Allinger, N. L.; Fermann, J. T.; Allen, W. D.; Schaefer, H. F. The Torsional Conformations of Butane: Definitive Energetics from Ab Initio Methods. *J. Chem. Phys.* **1997**, *106*, 5143−5150.
(69) Schuurman, M. S.; Muir, S. R.; Allen, W. D.; Schaefer, H. F. Toward Subchemical Accuracy in Computational Thermochemistry: Focal Point Analysis of the Heat of Formation of NCO and H,N,C,O Isomers. *J. Chem. Phys.* **2004**, *120*, 11586−11599.
(70) Sylvetsky, N.; Peterson, K. A.; Karton, A.; Martin, J. M. L. Toward a W4-F12 Approach: Can Explicitly Correlated and Orbital-Based Ab Initio CCSD(T) Limits Be Reconciled? *J. Chem. Phys.* **2016**, *144*, 214101.

https://dx.doi.org/10.1021/acs.jpca.0c09526
J. Phys. Chem. A 2021, 125, 1301−1324

(71) Almlöf, J.; Taylor, P. R. General Contraction of Gaussian-Basis Sets.I. Atomic Natural Orbitals for 1st-Row and 2nd-Row Atoms. *J. Chem. Phys.* **1987**, *86*, 4070−4077.
(72) Martin, J. M. L.; Taylor, P. R.; Lee, T. J. The Harmonic Frequencies of Benzene. A Case for Atomic Natural Orbital Basis Sets. *Chem. Phys. Lett.* **1997**, *275*, 414−422.
(73) McCaslin, L.; Stanton, J. Calculation of Fundamental Frequencies for Small Polyatomic Molecules: A Comparison Between Correlation Consistent and Atomic Natural Orbital Basis Sets. *Mol. Phys.* **2013**, *111*, 1492−1496.
(74) Gaw, J. F.; Yamaguchi, Y.; Schaefer, H. F.; Handy, N. C. Generalization of Analytic Energy 3rd Derivatives for the RHF Closed-Shell Wave-Function - Derivative Energy and Integral Formalisms and the Prediction of Vibration-Rotation Interaction Constants. *J. Chem. Phys.* **1986**, *85*, 5132−5142.
(75) Colwell, S. M.; Jayatilaka, D.; Maslen, P. E.; Amos, R. D.; Handy, N. C. Higher Analytic Derivatives 0.1. A New Implementation for the 3rd Derivative of the SCF Energy. *Int. J. Quantum Chem.* **1991**, *40*, 179−199.
(76) Maslen, P. E.; Jayatilaka, D.; Colwell, S. M.; Amos, R. D.; Handy, N. C. Higher Analytic Derivatives 0.2. The 4th Derivative of Self-Consistent-Field Energy. *J. Chem. Phys.* **1991**, *95*, 7409−7417.
(77) Ringholm, M.; Jonsson, D.; Bast, R.; Gao, B.; Thorvaldsen, A. J.; Ekstrom, U.; Helgaker, T.; Ruud, K. Analytic Cubic and Quartic Force Fields Using Density-Functional Theory. *J. Chem. Phys.* **2014**, *140*, 034103.
(78) Breidung, J.; Thiel, W.; Gauss, J.; Stanton, J. F. Anharmonic Force Fields from Analytic CCSD(T) Second Derivatives: HOF and F_2O. *J. Chem. Phys.* **1999**, *110*, 3687−3696.
(79) Gauss, J.; Stanton, J. F. Analytic CCSD(T) Second Derivatives. *Chem. Phys. Lett.* **1997**, *276*, 70−77.
(80) Matthews, D. A. Accelerating the Convergence of Higher-Order Coupled-Cluster Methods II: Coupled-Cluster Λ Equations and Dynamic Damping. *Mol. Phys.* **2020**, *118*, e1757774.
(81) M., Kállay; Rolik, Z.; Csontos, J.; Nagy, P.; Samu, G.; Mester, D.; Ladjánszki, I.; Szegedy, L.; Ladóczki, B.; Petrov, K.; et al. *MRCC, a quantum chemical program suite*. Rolik, Z.; Szegedy, L.; Ladjánszki, I.; Ladóczki, B.; Kállay, M. *J. Chem. Phys.* **2013**, *139*, 094105. See also:www.mrcc.hu.
(82) Kallay, M.; Nagy, P. R.; Mester, D.; Rolik, Z.; Samu, G.; Csontos, J.; Csoka, J.; Szabo, P. B.; Gyevi-Nagy, L.; Hegely, B.; et al. The MRCC Program System: Accurate Quantum Chemistry from Water to Proteins. *J. Chem. Phys.* **2020**, *152*, 074107.
(83) Allen, W. D.; Csaszar, A. G. On the Ab Initio Determination of Higher-Order Force-Constants at Nonstationary Reference Geometries. *J. Chem. Phys.* **1993**, *98*, 2983−3015.
(84) Pulay, P.; Fogarasi, G.; Pongor, G.; Boggs, J. E.; Vargha, A. Combination of Theoretical Ab Initio and Experimental Information to Obtain Reliable Harmonic Force-Constants - Scaled Quantum-Mechanical (SQM) Force-Fields for Glyoxal, Acrolein, Butadiene, Formaldehyde, and Ethylene. *J. Am. Chem. Soc.* **1983**, *105*, 7037−7047.
(85) Davisson, J. L.; Brinkmann, N. R.; Polik, W. F. Accurate and Efficient Calculation of Excited Vibrational States from Quartic Potential Energy Surfaces. *Mol. Phys.* **2012**, *110*, 2587−2598.
(86) Willetts, A.; Gaw, J. F.; Handy, N. C.; Carter, S. A Study of the Ground Electronic State of Hydrogen Peroxide. *J. Mol. Spectrosc.* **1989**, *135*, 370−388.
(87) Schneider, H.; Vogelhuber, K. M.; Schinle, F.; Stanton, J. F.; Weber, J. M. Vibrational Spectroscopy of Nitroalkane Chains Using Electron Autodetachment and Ar Predissociation. *J. Phys. Chem. A* **2008**, *112*, 7498−7506.
(88) Franke, P. R.; Brice, J. T.; Moradi, C. P.; Schaefer, H. F.; Douberly, G. E. Ethyl + O_2 in Helium Nanodroplets: Infrared Spectroscopy of the Ethylperoxy Radical. *J. Phys. Chem. A* **2019**, *123*, 3558−3568.
(89) Klatt, G.; Willets, A.; Handy, N. C. Anharmonic Effects in the Infrared Spectrum of SiH_3Br — An Ab Initio Study. *Chem. Phys. Lett.* **1996**, *249*, 272−278.
(90) Begue, D.; Carbonniere, P.; Pouchan, C. Calculations of Vibrational Energy Levels by Using a Hybrid Ab Initio and DFT Quartic Force Field: Application to Acetonitrile. *J. Phys. Chem. A* **2005**, *109*, 4611−4616.
(91) Dargelos, A.; Karamanis, P.; Pouchan, C. Theoretical Investigation of the Infrared Spectrum of 5-Bromo-2,4-Pentadiyne Nitrile from a CCSD(T)/B3LYP Anharmonic Potential. *ChemPhysChem* **2018**, *19*, 822−826.
(92) Begue, D.; Benidar, A.; Pouchan, C. The Vibrational Spectra of Vinylphosphine Revisited: Infrared and Theoretical Studies from CCSD(T) and DFT Anharmonic Potential. *Chem. Phys. Lett.* **2006**, *430*, 215−220.
(93) Rosnik, A. M.; Polik, W. F. VPT2+K Spectroscopic Constants and Matrix Elements of the Transformed Vibrational Hamiltonian of a Polyatomic Molecule with Resonances Using Van Vleck Perturbation Theory. *Mol. Phys.* **2014**, *112*, 261−300.
(94) Lehmann, K. K. Beyond the χ-K Relations - Calculations of 1−1 and 2−2 Resonance Constants with Application to HCN and DCN. *Mol. Phys.* **1989**, *66*, 1129−1137.
(95) Darling, B. T.; Dennison, D. M. The Water Vapor Molecule. *Phys. Rev.* **1940**, *57*, 128−139.
(96) Martin, J. M. L.; Taylor, P. R. Accurate Ab Initio Quartic Force Field for *trans*-HNNH and Treatment of Resonance Polyads. *Spectrochim. Acta, Part A* **1997**, *53*, 1039−1050.
(97) Bouwens, R. J.; Hammerschmidt, J. A.; Grzeskowiak, M. M.; Stegink, T. A.; Yorba, P. M.; Polik, W. F. Pure Vibrational Spectroscopy of S_0 Formaldehyde by Dispersed Fluorescence. *J. Chem. Phys.* **1996**, *104*, 460−479.
(98) Morgan, W. J.; Matthews, D. A.; Ringholm, M.; Agarwal, J.; Gong, J. Z.; Ruud, K.; Allen, W. D.; Stanton, J. F.; Schaefer, H. F. Geometric Energy Derivatives at the Complete Basis Set Limit: Application to the Equilibrium Structure and Molecular Force Field of Formaldehyde. *J. Chem. Theory Comput.* **2018**, *14*, 1333−1350.
(99) Amos, R. D.; Handy, N. C.; Green, W. H.; Jayatilaka, D.; Willetts, A.; Palmieri, P. Anharmonic Vibrational Properties of CH_2F_2: A Comparison of Theory and Experiment. *J. Chem. Phys.* **1991**, *95*, 8323−8336.
(100) Misiewicz, J. P.; Moore, K. B.; Franke, P. R.; Morgan, W. J.; Turney, J. M.; Douberly, G. E.; Schaefer, H. F. Sulfurous and Sulfonic Acids: Predicting the Infrared Spectrum and Setting the Surface Straight. *J. Chem. Phys.* **2020**, *152*, 024302.
(101) Pullen, G. T.; Franke, P. R.; Lee, Y. P.; Douberly, G. E. Infrared Spectroscopy of Propene in Solid *para*-Hydrogen and Helium Droplets: The Role of Matrix Shifts in the Analysis of Anharmonic Resonances. *J. Mol. Spectrosc.* **2018**, *354*, 7−14.
(102) Brown, A. R.; Brice, J. T.; Franke, P. R.; Douberly, G. E. Infrared Spectrum of Fulvenallene and Fulvenallenyl in Helium Droplets. *J. Phys. Chem. A* **2019**, *123*, 3782−3792.
(103) Franke, P. R.; Douberly, G. E. Rotamers of Isoprene: Infrared Spectroscopy in Helium Droplets and Ab Initio Thermochemistry. *J. Phys. Chem. A* **2018**, *122*, 148−158.
(104) Tabor, D. P.; Hewett, D. M.; Bocklitz, S.; Korn, J. A.; Tomaine, A. J.; Ghosh, A. K.; Zwier, T. S.; Sibert, E. L. Anharmonic Modeling of the Conformation-Specific IR Spectra of Ethyl, *n*-Propyl, and *n*-Butylbenzene. *J. Chem. Phys.* **2016**, *144*, 224310.
(105) Mackie, C. J.; Candian, A.; Huang, X. C.; Maltseva, E.; Petrignani, A.; Oomens, J.; Buma, W. J.; Lee, T. J.; Tielens, A. G. G. M. The Anharmonic Quartic Force Field Infrared Spectra of Hydrogenated and Methylated PAHs. *Phys. Chem. Chem. Phys.* **2018**, *20*, 1189−1197.
(106) Mackie, C. J.; Candian, A.; Huang, X. C.; Maltseva, E.; Petrignani, A.; Oomens, J.; Mattioda, A. L.; Buma, W. J.; Lee, T. J.; Tielens, A. G. G. M. The Anharmonic Quartic Force Field Infrared Spectra of Five Non-Linear Polycyclic Aromatic Hydrocarbons: Benz[a]anthracene, Chrysene, Phenanthrene, Pyrene, and Triphenylene. *J. Chem. Phys.* **2016**, *145*, 084313.
(107) Maltseva, E.; Petrignani, A.; Candian, A.; Mackie, C. J.; Huang, X. C.; Lee, T. J.; Tielens, A.; Oomens, J.; Buma, W. J. High-Resolution IR Absorption Spectroscopy of Polycyclic Aromatic Hydrocarbons: The Realm of Anharmonicity. *Astrophys. J.* **2015**, *814*, 23.

https://dx.doi.org/10.1021/acs.jpca.0c09526
J. Phys. Chem. A 2021, 125, 1301−1324

(108) Mackie, C. J.; Candian, A.; Huang, X. C.; Maltseva, E.; Petrignani, A.; Oomens, J.; Buma, W. J.; Lee, T. J.; Tielens, A. G. G. M. The Anharmonic Quartic Force Field Infrared Spectra of Three Polycyclic Aromatic Hydrocarbons: Naphthalene, Anthracene, and Tetracene. *J. Chem. Phys.* **2015**, *143*, 224314.

NOTE ADDED AFTER ASAP PUBLICATION

Due to a production error, this paper was published on the Web January 28, 2021, with an error in equation 76, and equations 48−77 incorrectly labeled as 49−78. The corrected version was reposted on January 29, 2021.

https://dx.doi.org/10.1021/acs.jpca.0c09526
J. Phys. Chem. A 2021, 125, 1301−1324